R-778

FOUR-BODY TRAJECTORY OPTIMIZATION

by

C. L. Pu and T. N. Edelbaum

December 1973

Final Report on NGR 22-009-207

Supplement No. 6

The Charles Stark Draper Laboratory, Inc.

Cambridge, Massachusetts 02139

R-778

FOUR-BODY TRAJECTORY OPTIMIZATION

C. L. Pu and T. N. Edelbaum

Final Report on NGR 22-009-207
Supplement No. 6

December 1973

THE CHARLES STARK DRAPER LABORATORY, INC.
CAMBRIDGE, MASSACHUSETTS 02139

Approved: David G. Hoag

ACKNOWLEDGEMENT

This report was prepared under DSR 56-40024, sponsored by the Goddard Space Flight Center, National Aeronautics and Space Administration through Grant NGR 22-009-207, Supplement No. 6. The authors wish to thank Robert Farquhar and Vearl Huff for their active interest in this project. The authors would also like to thank L. D'Amario for helpful discussions and advice.

ABSTRACT

The first part of this report presents a collection of typical 3-body trajectories from the L_1 libration point on the Sun-Earth line to the Earth. These trajectories in the Sun-Earth system may be grouped into four distinct families which differ in the transfer time and ΔV requirements. Also included are curves showing the variations of ΔV with respect to transfer time and typical 2 and 3-impulse primer vector histories.

The second part of the report deals with the development of a 4-body trajectory optimization program to compute fuel optimal trajectories between the Earth and a point in the Sun-Earth-Moon system. It presents methods for generating fuel optimal 2-impulse trajectories which may originate at the Earth or a point in space and fuel optimal 3-impulse trajectories between 2 points in space. The extrapolation of the state vector and the computation of the state transition matrix are accomplished by the Stumpff-Weiss method. The cost and constraint gradients are computed analytically in terms of the terminal state and the state transition matrix. The 4-body Lambert problem is solved by using the Newton-Raphson method. An accelerated gradient projection method is used to optimize a 2-impulse trajectory with terminal constraint. The Davidon's Variance Method is used both in the accelerated gradient projection method and the outer loop of a 3-impulse trajectory optimization problem. This method is preferred over many others mainly because it does not require a one-dimensional search. Several well-known methods which have been successful in solving 2-body trajectory optimization problems perform poorly in the 4-body system. A brief qualitative comparison of these methods is given.

An example of a 4-body 2-impulse transfer from the L_1 libration point to the Earth is included. The difference between this trajectory and a 3-body trajectory of the same transfer is readily discernable.

Page Intentionally Left Blank

TABLE OF CONTENTS

		Page
INTRODUCTION		1
PART I	EXAMPLES OF THREE-BODY TRAJECTORIES	4
	I.1 Generation of Three-Body Trajectories	5
	I.2 Examples of Typical 3-Body Trajectories from L_1 to Earth	6
PART II	FOUR-BODY TRAJECTORY OPTIMIZATION	20
	II.1 General	21
	II.2 Coordinate System	21
	II.3 Integration	21
	II.3.1 Stumpff-Weiss Method	22
	II.4 Structure	26
	II.4.1 Two-Impulse Transfer from Earth to a Point in Space	31
	II.4.2 Two-Impulse Transfer from a Point in Space to Earth	36
	II.4.3 Three-Impulse Transfer	40
	II.5 Iterations	51
	II.5.1 Evaluation of Iterations	52
	II.5.2 Recommended Iterations	54
	II.6 An Example of a Four-Body Two-Impulse Transfer	55
REFERENCES		60
APPENDIX A		63
APPENDIX B		65

INTRODUCTION

This report is divided into two parts. The first part is a collection of typical 3-body trajectories from the L_1 libration point on the Sun-Earth line to the earth. They are generated using routines based on the program developed by D'Amario[1]. The extrapolation of the state vector is accomplished by the Wilson's version of the multi-conic method[8, 9]. These trajectories in the Sun-Earth system may be grouped into four distinct families which differ in the transfer time and ΔV requirement. The effect of the moon is approximated by adding the mass of the moon to the mass of the earth and increasing the initial parking orbit radius so that the velocity is the same as in a 100 n. m. earth orbit. Also included in the first part are curves showing the variations of ΔV with respect to transfer time and typical two and three-impulse primer vector histories. The experience gained in solving the 3-body trajectory optimization problems has been most valuable in the subsequent development of the 4-body trajectory optimization program.

The second part of this report deals with the development of a comprehensive program to compute fuel optimal 4-body trajectories between the earth and some point in the Sun-Earth-Moon system. The moon is treated as a separate entity. The basic building blocks of the program are the integrator and the iterators. The manner in which these building blocks are connected depends on the selection of the dependent and independent variables. The integrator uses the Stumpff-Weiss method[10, 11] to extrapolate the state vector and to compute the state transition matrix. An important feature is that the cost and constraint gradients can be computed analytically in terms of the terminal state and the state transition matrix. This method does not require the switching of coordinates and generates its own ephemerides. The iterators solve the boundary value problems to satisfy terminal conditions or to optimize ΔV with or without terminal constraints.

The generation of a 4-body fuel optimal trajectory is considerably more difficult and time-consuming than in the 2-body system mainly because of the increased difficulty in solving the Lambert problem. In

a 4-body 2-impulse transfer it is generally necessary to go through a search process to obtain an initial estimate of the required velocity. If the initial estimate is reasonably good so that the terminal miss is small, an iterative solution of the boundary value problem will converge to the required velocity. If the boundary conditions and/or the transfer time are changed, the required velocity for the perturbed trajectory may be obtained by iterating on the Lambert solution for the reference trajectory provided that the changes are kept small. In general, the solution of the Lambert problem will require several iterations, each involving a costly function evaluation (the extrapolation of the state vector and the state transition matrix). On the other hand, the computation of the gradient in terms of the terminal state and the state transition matrix is trivial.

A number of iterators which have been successful in solving 2-body trajectory optimization problems perform poorly in the 4-body system. They either require too many function evaluations or just fail to converge. The selection of iterators is thus of major importance.

Some reduction in computer time is possible by a judicious choice of the independent variables. For instance, the classical choice of the independent variables to optimize ΔV in a 2-body 3-impulse transfer is the position and time of the interior impulse[2, 3]. The gradient of ΔV with respect to the independent variables may be expressed in terms of the time derivative of the primer vector. Since the solution of the 2-body Lambert problem is a single step process, there is no inner loop of importance. When this approach is applied to a 4-body problem, it would require the solution of two difficult inner loop Lambert problems to satisfy constraints at two places and an outer loop to optimize ΔV. The 4-body problem is highly non-linear in that the inner loops will fail to converge unless the changes in the interior impulse position and time as generated by the outer loop are heavily constrained. As a result, the progress to a converged solution tends to be very slow.

In view of the fact that the reference and the perturbed trajectories are required to satisfy the same boundary conditions, there are only

four degrees of freedom. Thus, a better approach is to iterate on the initial required velocity and the time of the interior impulse in the outer loop. The effect of this change is that one of the two inner loop Lambert problems is eliminated. The gradient of cost with respect to the new independent variables may be computed without computing the primer vector. This new approach results in a significant saving in computer time. To insure convergence the required change in the interior impulse position with respect to the reference trajectory for the remaining Lambert problem is introduced in increments rather than in one single step. After the problem has converged to a solution, the primer vector history is computed to determine whether the trajectory is optimal or an additional impulse is required.

The 4-body trajectory optimization program provides the capability to compute 2-impulse transfers between the earth and a point in space with or without optimization and 3-impulse fuel-optimal transfers between two points in space. The 2-impulse transfer may originate from the earth or a point in space. The terminal condition of a point to earth transfer may be either of a point to point type (PTP) or of a point to radius type (PTR). The initial condition of a transfer from the earth to a point in space is of a PTP type in which the initial position is also varied to optimize ΔV.

This report is concluded by showing an example of a 4-body 2-impulse transfer from the L_1 libration point to the earth. The transfer time is chosen to be the same as the typical loop type 3-body trajectory. The difference between the 4-body and 3-body trajectories is readily discernable.

PART I

EXAMPLES OF THREE-BODY TRAJECTORIES

I.1 Generation of Three-Body Trajectories

Both 2-impulse and 3-impulse trajectories in the 3-body system have been generated between the L_1 libration point on the Sun-Earth line and the earth. The motion of the earth is assumed to be circular around the sun. The trajectories of the earth and the vehicle are confined to the ecliptic. The 2-impulse transfer originates from the L_1 point and terminates at the earth with a given radius and zero radial velocity. The terminal radius corresponds to a parking orbit which would give the same circular velocity as in an 100 n. m. orbit after adding the mass of the moon to the mass of the earth.

The procedure used to generate a typical family of 2-impulse trajectories are as follows.

1. A magnitude of the required velocity at L_1 is selected and the direction relative to the Sun-Earth barycentric line is varied. The state vector is extrapolated to a prescribed terminal time using the Wilson's version of the multi-conic method[8]. The state transition matrix is computed along with the trajectory. A field of trajectories is generated in this manner. An initial estimate of the required velocity is obtained from the trajectory which has the smallest miss distance.
2. The constraint gradient is computed in terms of the terminal state and the state transition matrix. The Lambert problem is then solved by iterating on the initial velocity using the Newton-Raphson method until the desired terminal conditions are satisfied.
3. The terminal time is varied and the Lambert problem is re-solved using the required velocity of the reference trajectory as the initial estimate. A parabola fit is used to extrapolate the required velocity from three adjacent Lambert solutions.
4. The variations of ΔV with respect to flight time is plotted. The primer vector history of the two-impulse transfer which requires the minimum ΔV with respect to the flight time is examined.

5. If the magnitude of the primer vector history exceeds one, a three-impulse trajectory is generated using a method similar to the one described under Part II.

I.2 Examples of Typical 3-Body Trajectories from L_1 to Earth

The 3-body trajectories may be grouped into four distinct families. Typical trajectories of these families are summarized in Table I.

The first three families of trajectories have corresponding trajectories found by previous investigators for moon to L_2 transfers in the Earth-Moon system. The last family is new.

TABLE I

Typical 3-Body Trajectories

Family	Typical 2-Impulse Trajectories				ΔV vs Time	Primer Vector History for 3-Impulse Trajectory
	Transfer Time (Day)	Traj.	ΔV (m/s)	Primer Vector History		
Fast (L_1 to leading edge of earth)	33.563	Fig. 1	454.446	Fig. 2	Fig. 5	Note 2
Fast (L_1 to trailing edge of earth)	35.563	Fig. 3	341.350	Fig. 4	Fig. 5	Note 2
Loop type	116.682	Fig. 6	272.137	Fig. 7	Fig. 8	Fig. 9
Double pass type	174.32	Fig. 10	203.34	Fig. 11	Fig. 12 Note 4	Note 3

NOTE:

1. Mass ratios used are shown in Appendix A.
2. The 2-impulse transfer is fuel-optimal. A third impulse is not required.
3. A converged solution to a 3-impulse transfer has not been obtained.
4. Extrapolation has not been carried out far enough to establish the flight time for minimum ΔV.

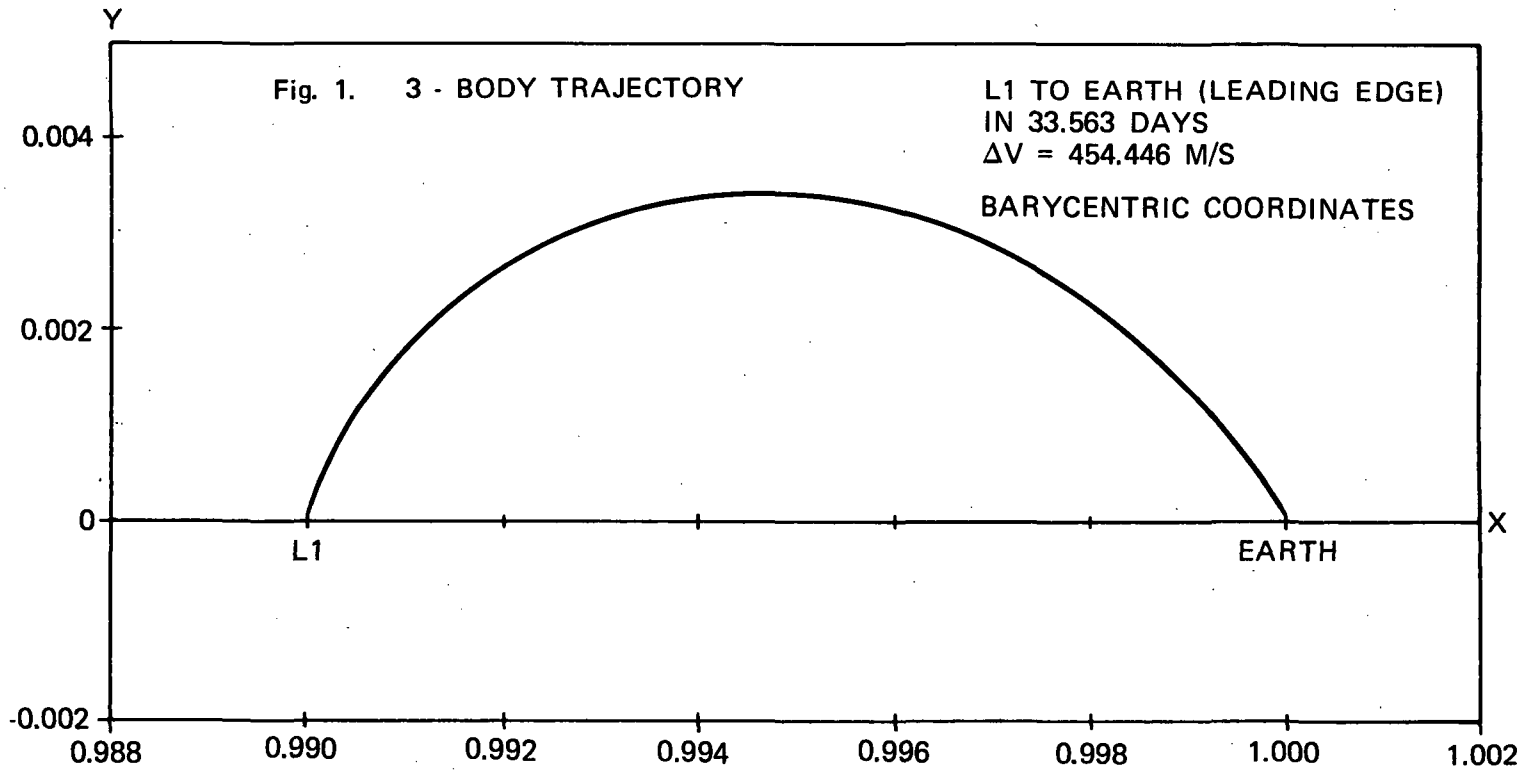
Y
Fig. 1. 3 - BODY TRAJECTORY
L1 TO EARTH (LEADING EDGE)
IN 33.563 DAYS
ΔV = 454.446 M/S
BARYCENTRIC COORDINATES
0.004
0.002
0
-0.002
L1
EARTH
X
0.988
0.990
0.992
0.994
0.996
0.998
1.000
1.002

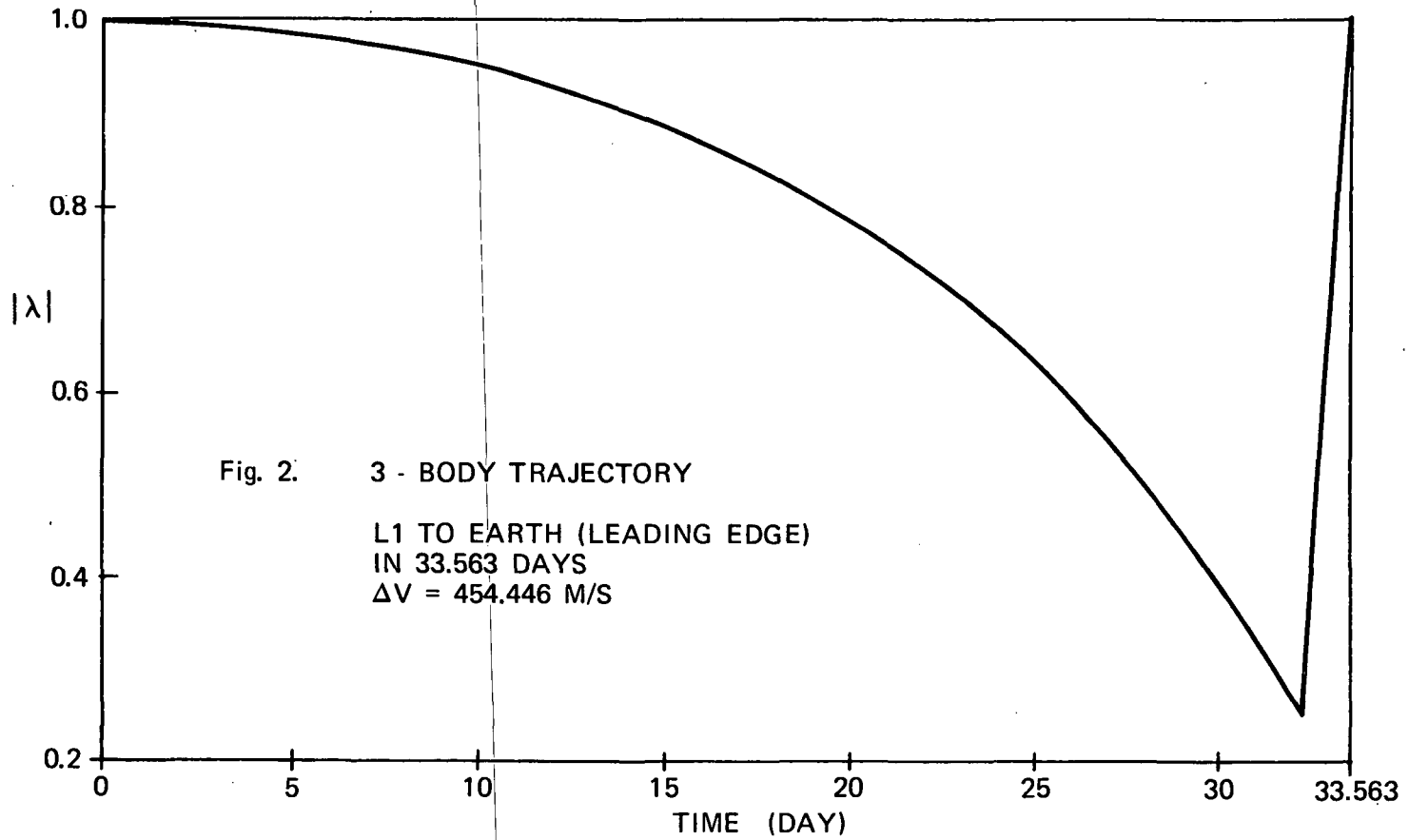

Fig. 2. 3 - BODY TRAJECTORY

L1 TO EARTH (LEADING EDGE)
IN 33.563 DAYS
ΔV = 454.446 M/S

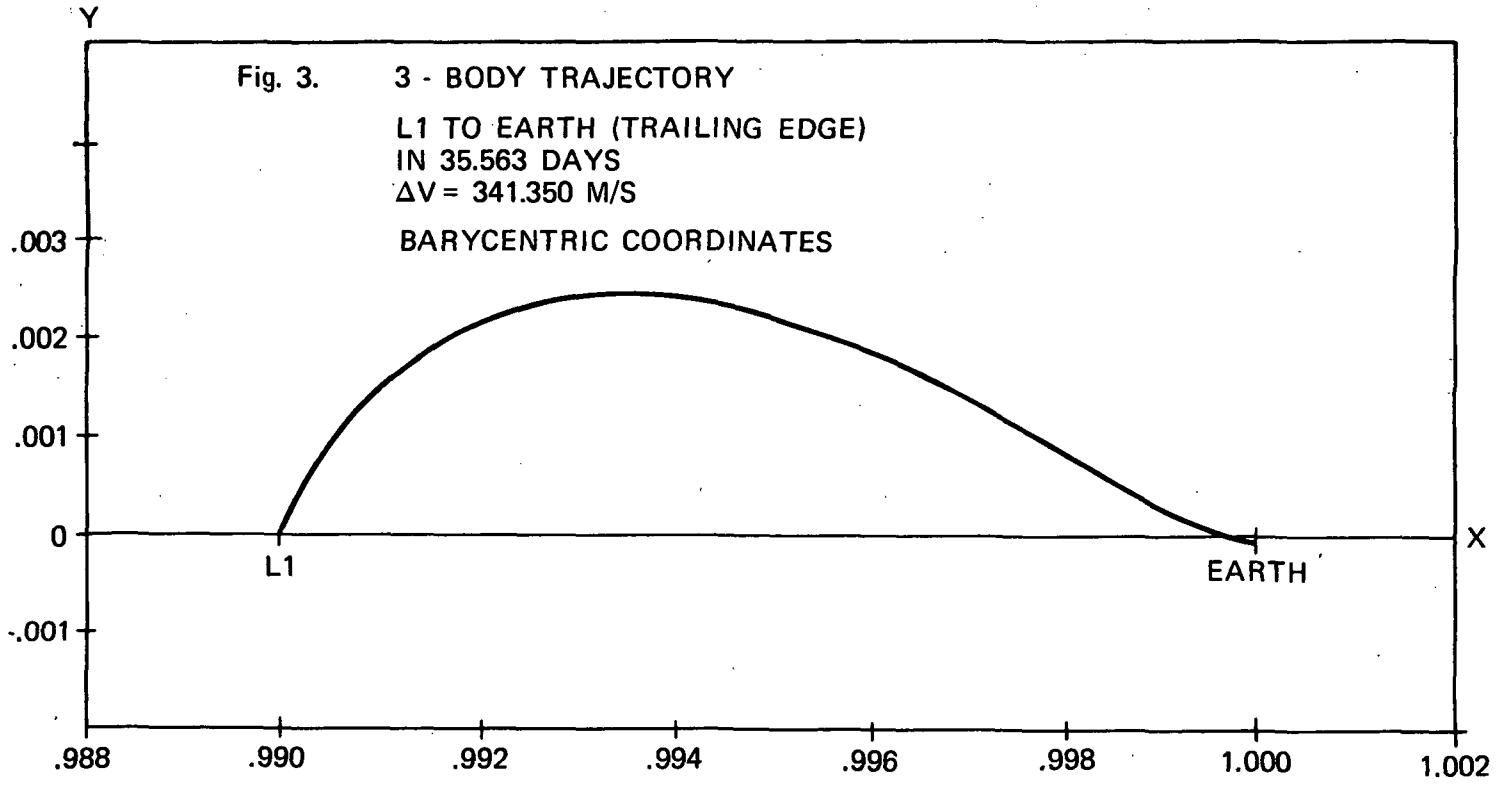
Y
Fig. 3. 3 - BODY TRAJECTORY
L1 TO EARTH (TRAILING EDGE)
IN 35.563 DAYS
ΔV = 341.350 M/S
BARYCENTRIC COORDINATES
.003
.002
.001
0
-.001
L1
EARTH
X
.988
.990
.992
.994
.996
.998
1.000
1.002

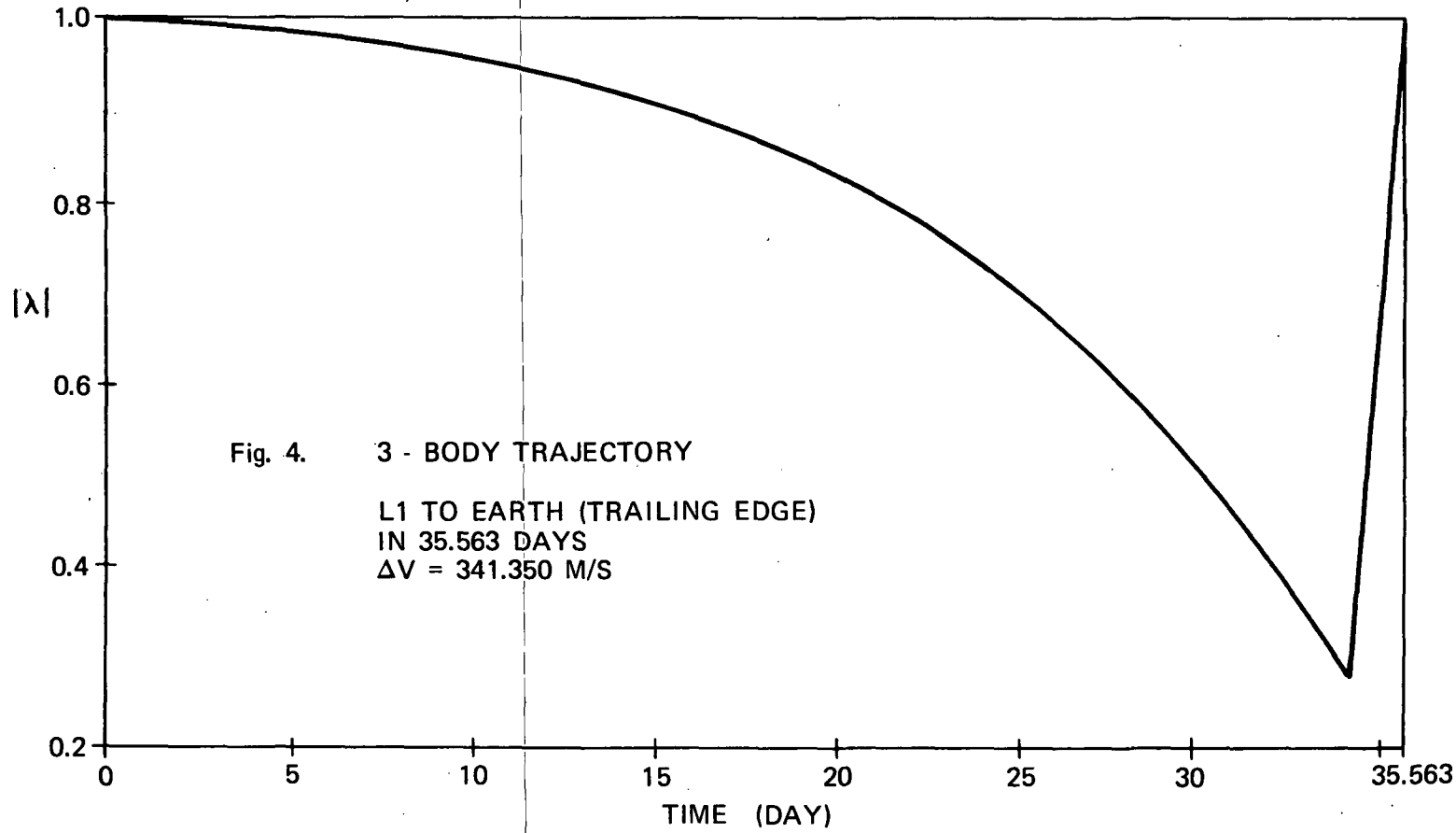

Fig. 4. 3 - BODY TRAJECTORY

L1 TO EARTH (TRAILING EDGE)
IN 35.563 DAYS
ΔV = 341.350 M/S

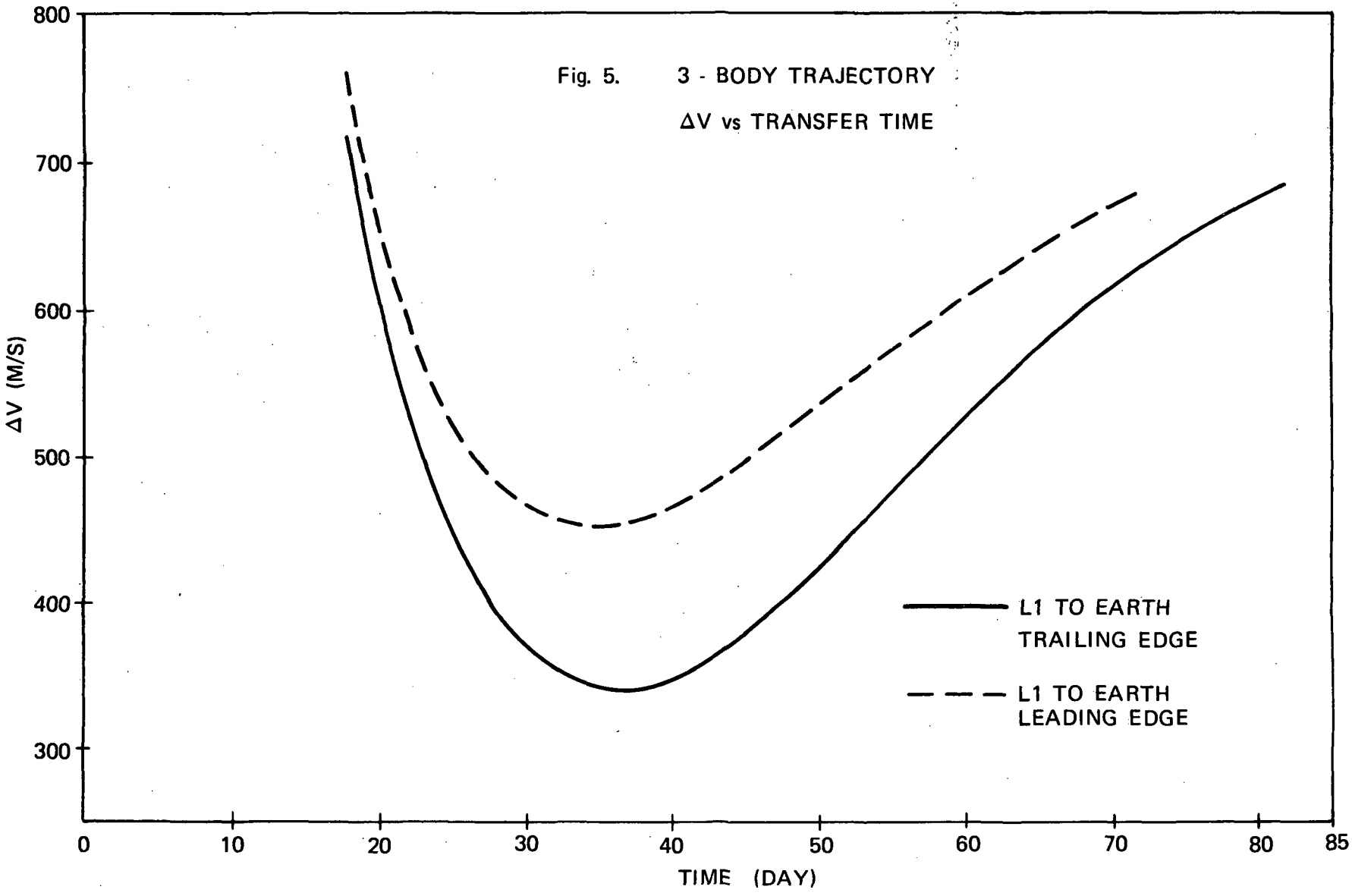

Fig. 5. 3 - BODY TRAJECTORY
ΔV vs TRANSFER TIME

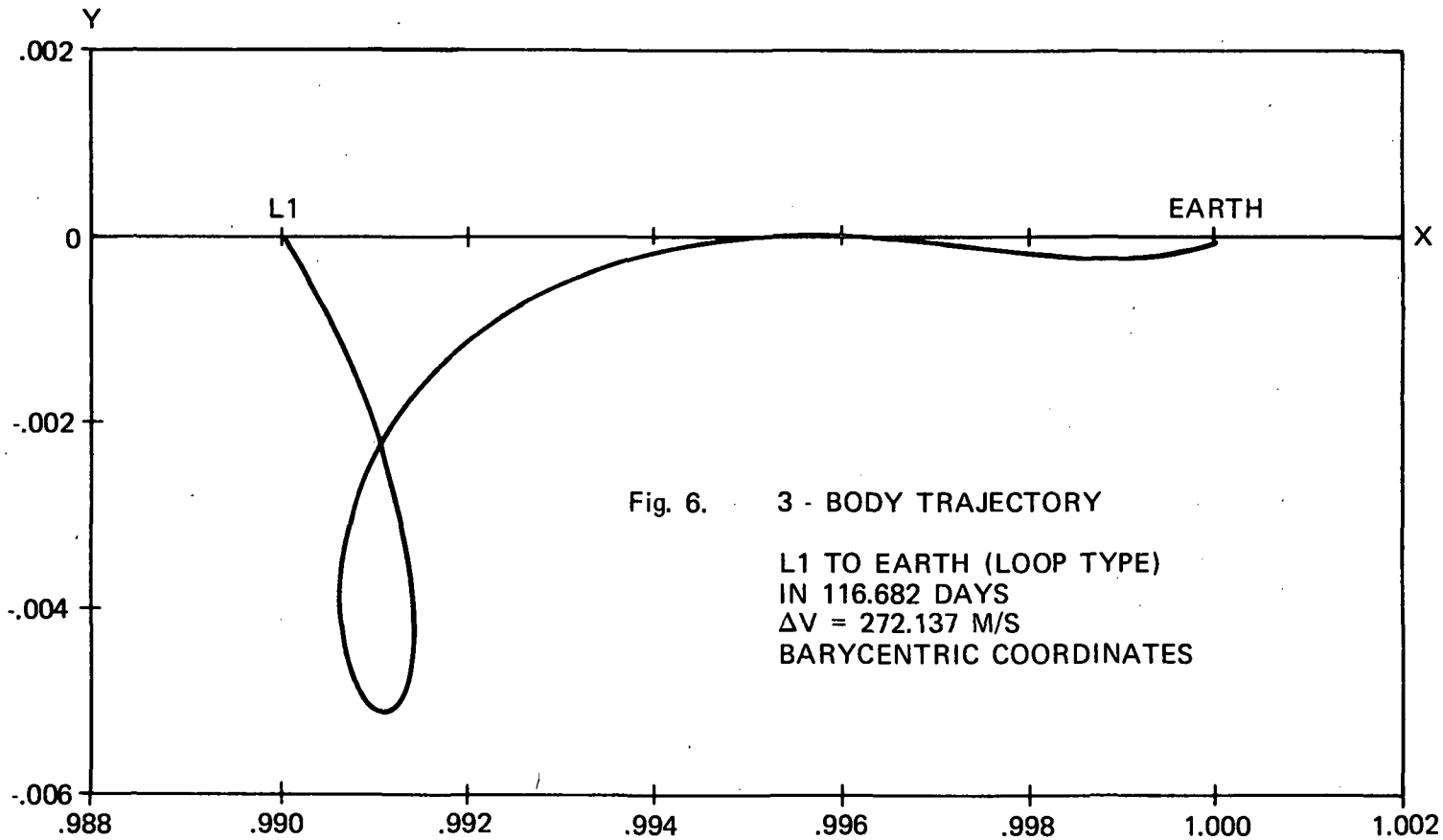

Fig. 6. 3 - BODY TRAJECTORY

L1 TO EARTH (LOOP TYPE)
IN 116.682 DAYS
ΔV = 272.137 M/S
BARYCENTRIC COORDINATES

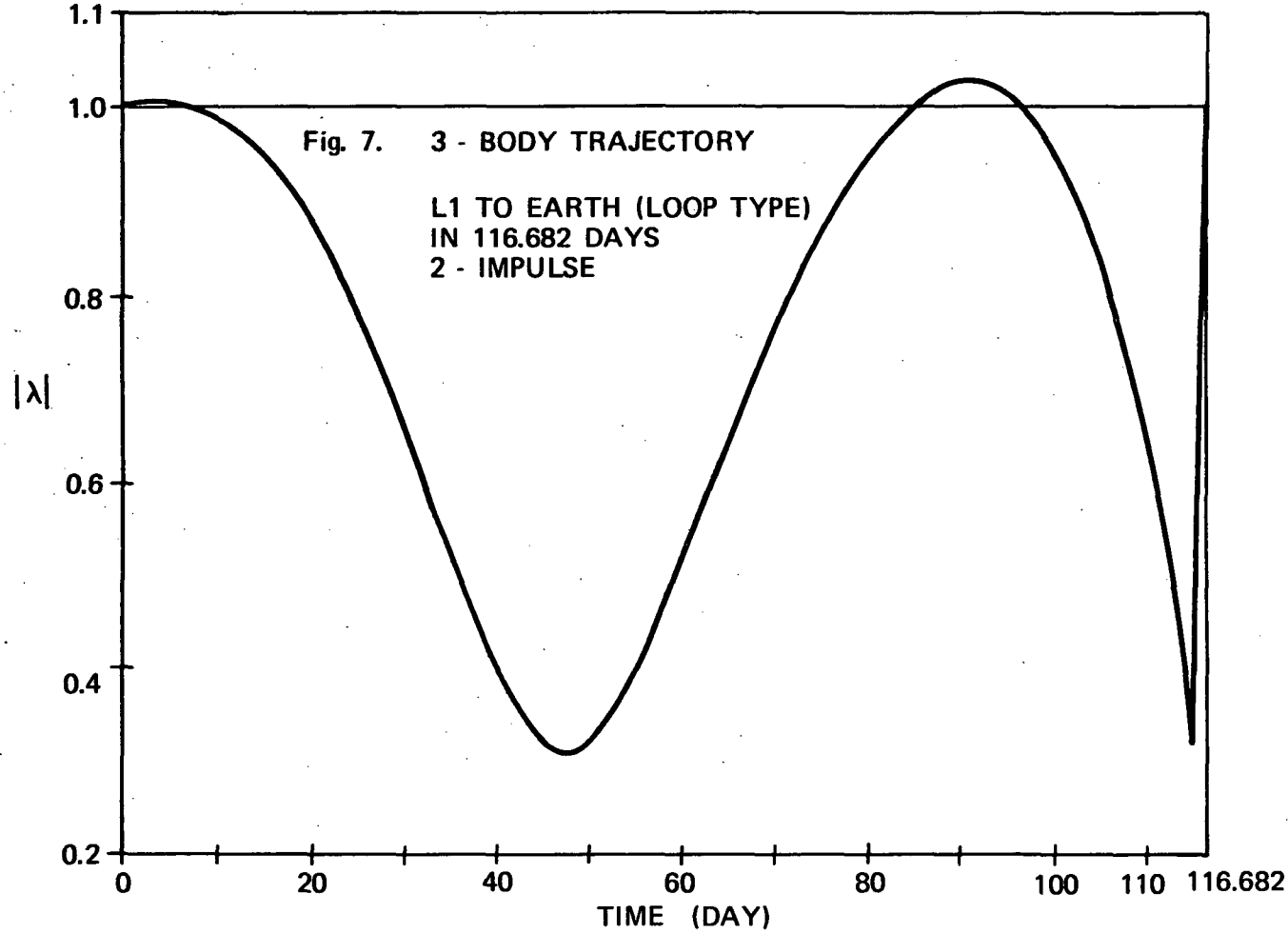
Fig. 7. 3 - BODY TRAJECTORY
L1 TO EARTH (LOOP TYPE)
IN 116.682 DAYS
2 - IMPULSE
1.1
1.0
0.8
0.6
0.4
0.2
|λ|
0
20
40
60
80
100
110
116.682
TIME (DAY)

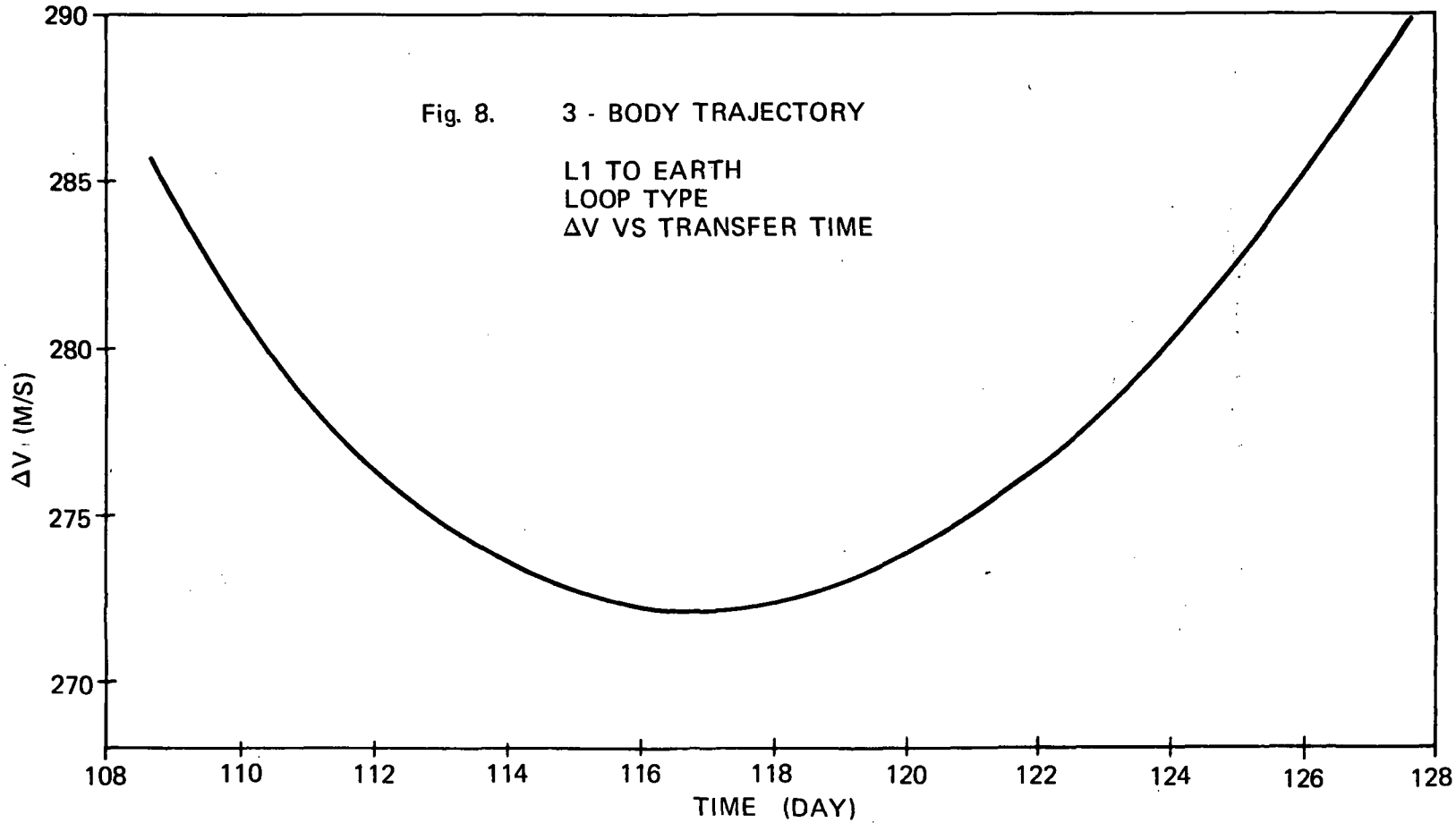

Fig. 8. 3 - BODY TRAJECTORY

L1 TO EARTH
LOOP TYPE
ΔV VS TRANSFER TIME

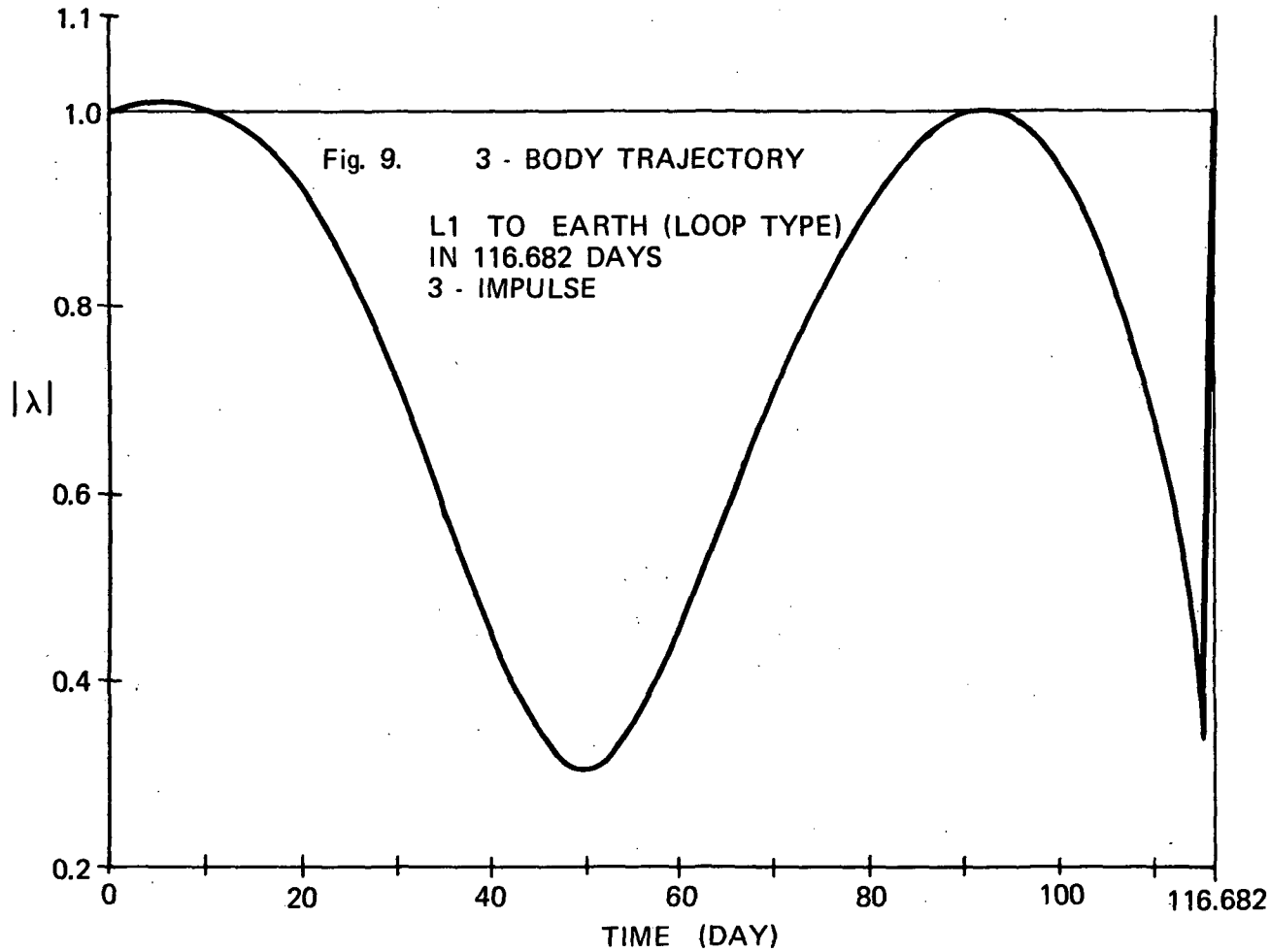
1.1
1.0
0.8
0.6
0.4
0.2
|λ|
0
20
40
60
80
100
116.682
TIME (DAY)
Fig. 9. 3 - BODY TRAJECTORY
L1 TO EARTH (LOOP TYPE)
IN 116.682 DAYS
3 - IMPULSE

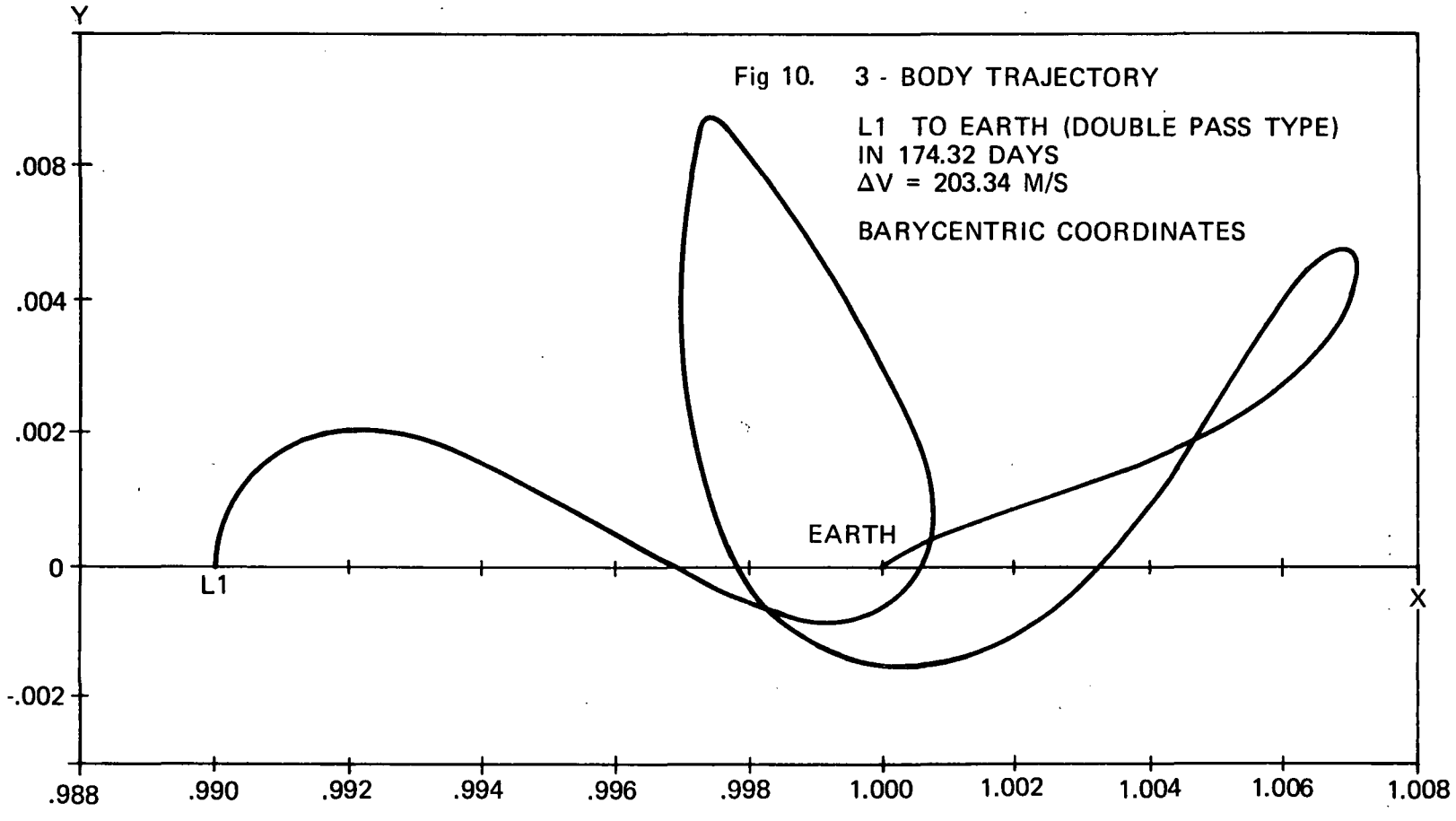

Fig 10. 3 - BODY TRAJECTORY

L1 TO EARTH (DOUBLE PASS TYPE)
IN 174.32 DAYS
ΔV = 203.34 M/S

BARYCENTRIC COORDINATES

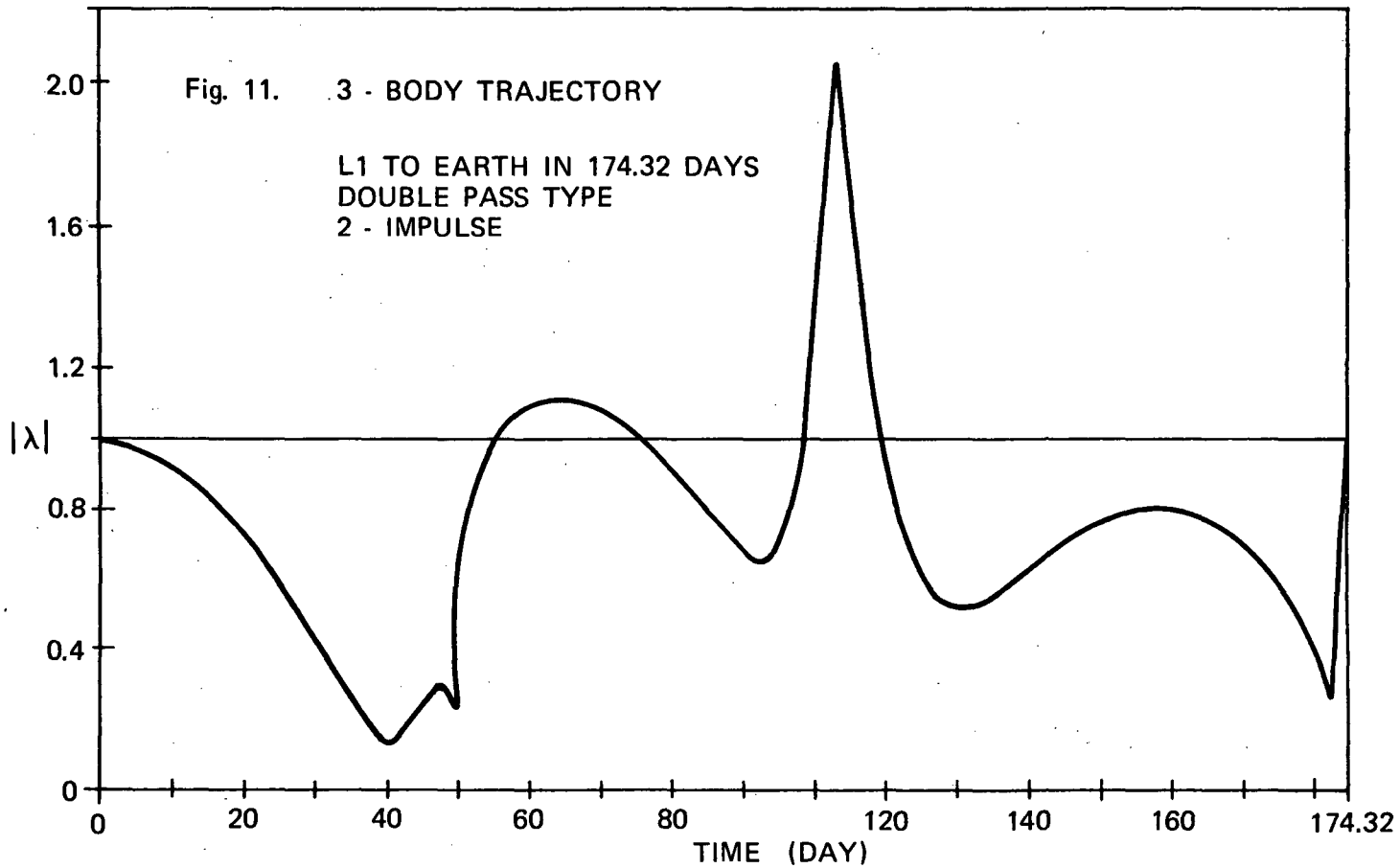
Fig. 11. 3 - BODY TRAJECTORY
L1 TO EARTH IN 174.32 DAYS
DOUBLE PASS TYPE
2 - IMPULSE
2.0
1.6
1.2
|λ|
0.8
0.4
0
0
20
40
60
80
120
140
160
174.32
TIME (DAY)

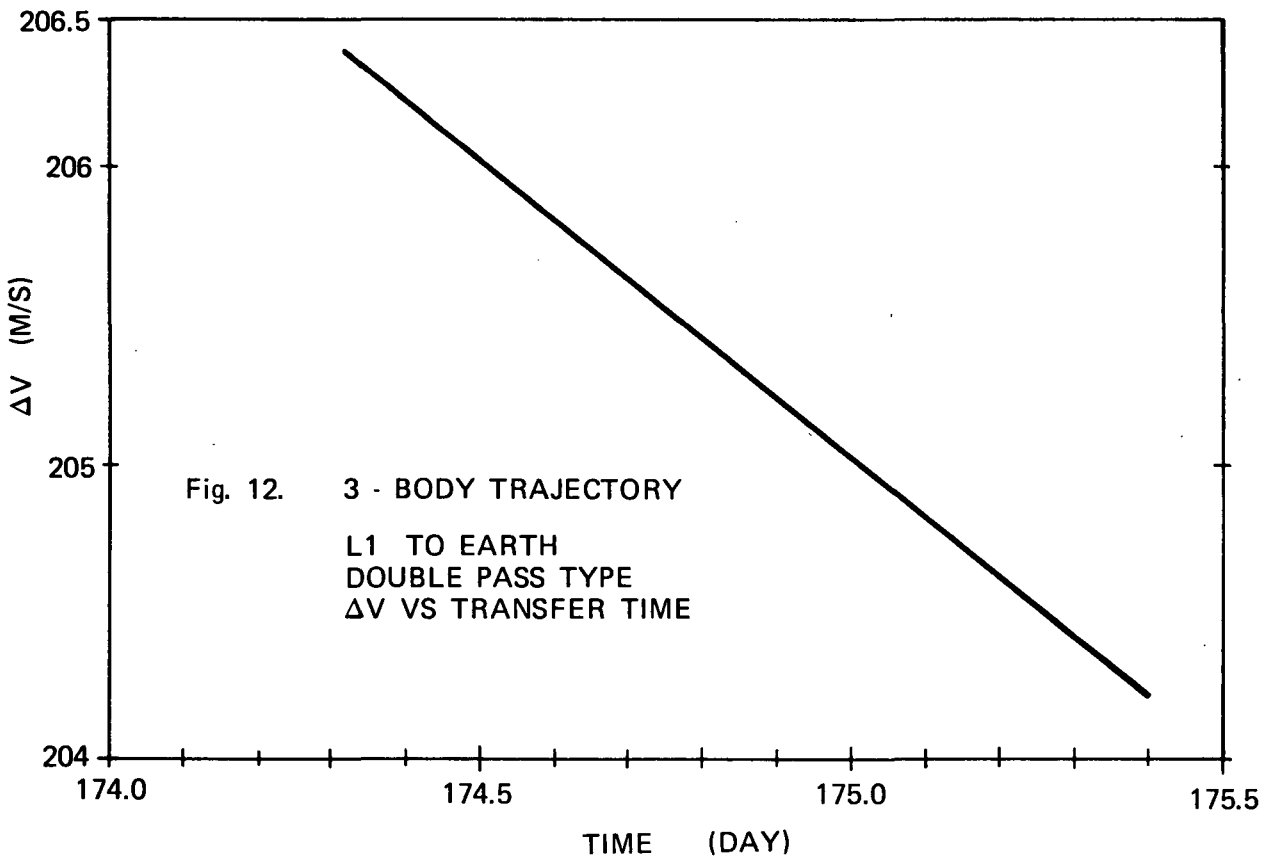

Fig. 12. 3 - BODY TRAJECTORY

L1 TO EARTH
DOUBLE PASS TYPE
ΔV VS TRANSFER TIME

PART II

FOUR-BODY TRAJECTORY OPTIMIZATION

II.1 General

The basic building blocks of the 4-body trajectory optimization program are the integrator and the iterators. The integrator is the routine to extrapolate state vector and compute the state transition matrix. The iterators are the routines to solve boundary value problems with or without optimization. The types of problems which will be encountered may be classified into three groups.

1. No optimization - Solution of Lambert problem to satisfy terminal constraint only.
2. Optimization only - Example - outer loop of a 3-impulse transfer
3. Optimization with constraints - Example - two-impulse transfer from the earth to a point in space

The structure of the program is determined by the choice of the dependent and independent variables.

II.2 Coordinate System

All coordinate systems are three dimensional, non-rotating, parallel Cartesian systems with their origins located at the center of mass of the body. The x-y plane of the sun-centered system lies in the ecliptic. The orientation of the axes in the ecliptic is not specified and will depend on the source which provides the ephemerides for the initial conditions. A possible choice, for example, is to require the x-axis to intersect the Vernal Equinox at the beginning of the nearest Besselian year.

II.3 Integrator

There are only two methods which are suitable for use in a 4-body trajectory optimization program. They are both multi-conic methods. The first version is due to Wilson[8] and the second version is due to Stumpff and Weiss[10]. The major difference between the two methods is that during each time step the former computes the two-body conics in sequence while the latter computes them in a parallel manner. In a 4-body space the Stumpff-Weiss method has the following advantages:

1. At each time step, no logic is required to determine the proper sequence of computation of the conics. While this is not a problem in a 3-body space, it introduces complications in a 4-body space.
2. The method generates its own ephemerides for the 4-body space. If the ephemerides are read, say, from a JPL tape, it is not possible to exclude the presence of the other bodies.

Input ephemerides are needed as initial conditions only. The required inputs are the initial positions and velocities of the earth, moon and vehicle with respect to the sun at the initial time and the mass ratios of the massive bodies.

II.3.1 Stumpff-Weiss Method[10]

The 4-body space is shown in Figure 13. The position and velocity vectors of a body are indicated by the second subscript with respect to another body indicated by the first subscript.

At each time step it is required to compute six two-body conics and three approximate perturbation vectors. From these conics and perturbation vectors are obtained six reference trajectories. The state transition matrix is computed from the two-body state transition matrices. The reference trajectories are in error equal to the remainders which will be computed every four time steps to indicate the errors but not used to correct the reference trajectories. This is because the computed state transition matrix is valid only for the reference trajectories. If the errors are too big, the user may decrease the step size or increase the number of steps accordingly.

At the first time step, the reference trajectories equal the true trajectories. At subsequent time step, the reference trajectories are used as inputs to generate the conics and the approximate perturbations.

The six conics will be generated using Goodyears routines[13]. They are denoted by:

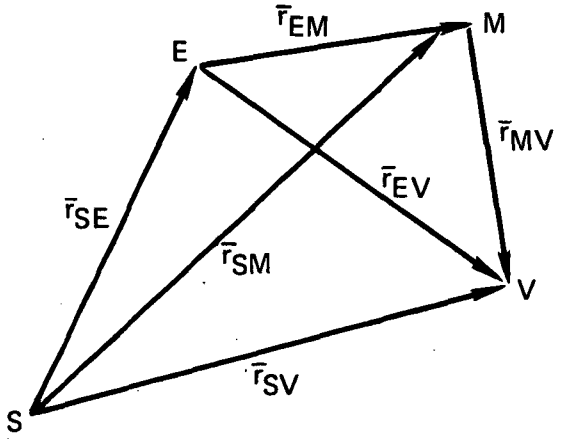

Fig. 13 4 - Body System

$$[\bar{p}_{i,\,j}] = ([\bar{r}_{i,\,j}], [\bar{v}_{i,\,j}])$$
$$i = S,\ E,\ M$$
$$j = E,\ M,\ V$$
$$i \neq j$$

The six reference trajectories are denoted by:

$$\bar{p}^{*}_{i,\,j} = (\bar{r}^{*}_{i,\,j},\ \bar{v}^{*}_{i,\,j})$$
$$i = S,\ E,\ M$$
$$j = E,\ M,\ V$$
$$i \neq j$$

The three approximate perturbations are given by equations below.

$$\bar{P}_{SV} = \frac{\mu_E}{\mu_S + \mu_E}\{[\bar{p}_{SE}] - J\,\bar{p}^{*}_{SE}(0)\} + \{[\bar{p}_{EV}] - J\,\bar{p}^{*}_{EV}(0)\}$$
$$+ \frac{\mu_M}{\mu_S + \mu_M}\{[\bar{p}_{SM}] - J\,\bar{p}^{*}_{SM}(0)\} + \{[\bar{p}_{MV}] - J\,\bar{p}^{*}_{MV}(0)\} \qquad (1)$$

$$\bar{P}_{SE} = \frac{\mu_M}{\mu_S + \mu_M}\{[\bar{p}_{SM}] - J\,\bar{p}^{*}_{SM}(0)\} - \frac{\mu_M}{\mu_M + \mu_E}\{[\bar{p}_{EM}] - J\,\bar{p}^{*}_{EM}(0)\}$$

$$\bar{P}_{SM} = \frac{\mu_E}{\mu_S + \mu_E}\{[\bar{p}_{SE}] - J\,\bar{p}^{*}_{SE}(0)\} + \frac{\mu_E}{\mu_E + \mu_M}\{[\bar{p}_{EM}] - J\,\bar{p}^{*}_{EM}(0)\}$$

where

μ_i = mass ratio, i = S, E, M

h = step size

$\bar{p}^{*}_{ij}(0)$ = reference trajectory at beginning of step

i = S, E, M

j = E, M, V

$i \neq j$

$$J = \begin{bmatrix} I_3 & hI_3 \\ 0_3 & I_3 \end{bmatrix}$$

The reference trajectory is computed from Equation (2).

$$\begin{aligned}
\bar{p}^{*}_{SV} &= [\bar{p}_{SV}] + \bar{P}_{SV} \\
\bar{p}^{*}_{SE} &= [\bar{p}_{SE}] + \bar{P}_{SE} \\
\bar{p}^{*}_{SM} &= [\bar{p}_{SM}] + \bar{P}_{SM} \\
\bar{p}^{*}_{EV} &= -\bar{p}^{*}_{SE} + \bar{p}^{*}_{SV} \\
\bar{p}^{*}_{MV} &= -\bar{p}^{*}_{SM} + \bar{p}^{*}_{SV} \\
\bar{p}^{*}_{EM} &= -\bar{p}^{*}_{SE} + \bar{p}^{*}_{SM}
\end{aligned} \tag{2}$$

The state transition matrix is computed from state transition matrices of two-body conics in Equation (3)[11].

$$\begin{aligned}
\varphi_h(t+h,\ t) &= \varphi_{SV}(t+h,\ t) + \varphi_{EV}(t+h,\ t) + \varphi_{MV}(t+h,\ t) - 2J \\
\varphi(t+h,\ t_o) &= \varphi_h(t+h,\ t)\ \varphi(t,\ t_o)
\end{aligned} \tag{3}$$

The errors or remainders in the reference trajectories propagate according to Equation (4).

$$\begin{aligned}
\ddot{\bar{R}}_{SV} &= \mu_S\, \bar{s}_{SV} + \mu_E\, (\bar{s}_{SE} + \bar{s}_{EV}) + \mu_M\, (\bar{s}_{SM} + \bar{s}_{MV}) \\
\ddot{\bar{R}}_{SE} &= (\mu_S + \mu_E)\, \bar{s}_{SE} + \mu_M\, (\bar{s}_{SM} - \bar{s}_{EM}) \\
\ddot{\bar{R}}_{SM} &= (\mu_S + \mu_M)\, \bar{s}_{SM} + \mu_E\, (\bar{s}_{SE} + \bar{s}_{EM})
\end{aligned} \tag{4}$$

where

$$\bar{s}_{ij} = \frac{[\bar{r}_{ij}]}{[|\bar{r}_{ij}|]^3} - \frac{\bar{r}_{ij}}{|\bar{r}_{ij}|^3} \tag{5}$$

$$i = S, E, M$$

$$j = E, M, V$$

$$i \neq j$$

Since we have used $\bar{r}^*_{ij}$ instead of the true $\bar{r}_{ij}$ in $\bar{s}_{ij}$, the error in $(\bar{s}_{ij} - \bar{s}^*_{ij})$ is h^4. Then the errors in $\ddot{\bar{R}}$ is also h^4 and the errors in $\bar{R}$ is h^6 if the remainders are used to correct the reference trajectories. The values of $\ddot{\bar{R}}$ for four time steps are saved and the remainders at every fourth step are computed using Stirling's five-point formulation shown in Equation 6[12].

$$\begin{aligned}
\dot{\bar{R}}(t_o + 4h) &= \frac{h}{45}[64\,\ddot{\bar{R}}(t_o + h) + 24\,\ddot{\bar{R}}(t_o + 2h) \\
&\quad + 64\,\ddot{\bar{R}}(t_o + 3h) + 14\,\ddot{\bar{R}}(t_o + 4h) \\
\bar{R}(t_o + 4h) &= \frac{h^2}{45}[192\,\ddot{\bar{R}}(t_o + h) + 48\,\ddot{\bar{R}}(t_o + 2h) \\
&\quad + 64\,\ddot{\bar{R}}(t_o + 3h)
\end{aligned} \tag{6}$$

where t_o = time at beginning of every 4 time steps.

II.4 Structure

The structure of the trajectory optimization program is strongly influenced by the choice of the dependent and independent variables. A particular choice determines how many integrators and iterators are required and how they are connected together.

In a two-impulse transfer, the logical choice is the required

velocity at the initial time. If the transfer time is fixed and the transfer originates from the earth, the initial position vector must also be iterated. The terminal constraint may be of a point to point (PTP) type or a point to radius (PTR) type. The PTR terminal consists of three components: the desired radial distance at earth, the desired radial velocity (usually zero), and the desired orbital inclination angle with respect to the ecliptic. The PTP terminal is the desired position vector. The two-impulse transfer is shown in Fig. 18 and 19.

In a three-impulse transfer, the problem is to perturb a reference trajectory in such a way that cost is reduced. Both the reference trajectory and the perturbed trajectory must satisfy the same PTP terminals.

In the classical method[2, 3], the independent variables are the position and time of the interior impulse ($\bar{r}_m$, t_m). It requires two inner loops to solve two Lambert problems to satisfy terminal conditions at t_m and t_f and an outer loop to change ($\bar{r}_m$, t_m) to reduce ΔV. This method was developed for two-body problems where the Lambert problem can be solved in one step. In the four-body problem the solution of the Lambert problem must be done in multiple steps and is very time consuming. In adapting the Optimum Multi-Impulse Rendezvous Program (OMIR)[4] to a four-body problem it was found that most of the computer time was spent in extrapolating the state vector and solving the Lambert problem in the one-dimensional search. Furthermore, the four-body transfer trajectory is very sensitive to changes in $\bar{r}_m$ and t_m. The Lambert problems will converge only when $\Delta\bar{r}_m$ and Δt_m are kept very small. The net effect is that the reduction in ΔV is small from one iteration to another.

The family of the three-impulse transfer trajectories has four degrees of freedom. It is then possible to change the outer loop independent variables from ($\bar{r}_m$, t_m) to ($\bar{v}_o$, t_m). In this choice, $\bar{r}_m$ is determined by $\bar{v}_o$ and t_m. It is only necessary to iterate on $\bar{v}_m^+$ to satisfy the terminal constraints. In other words, there is only one Lambert

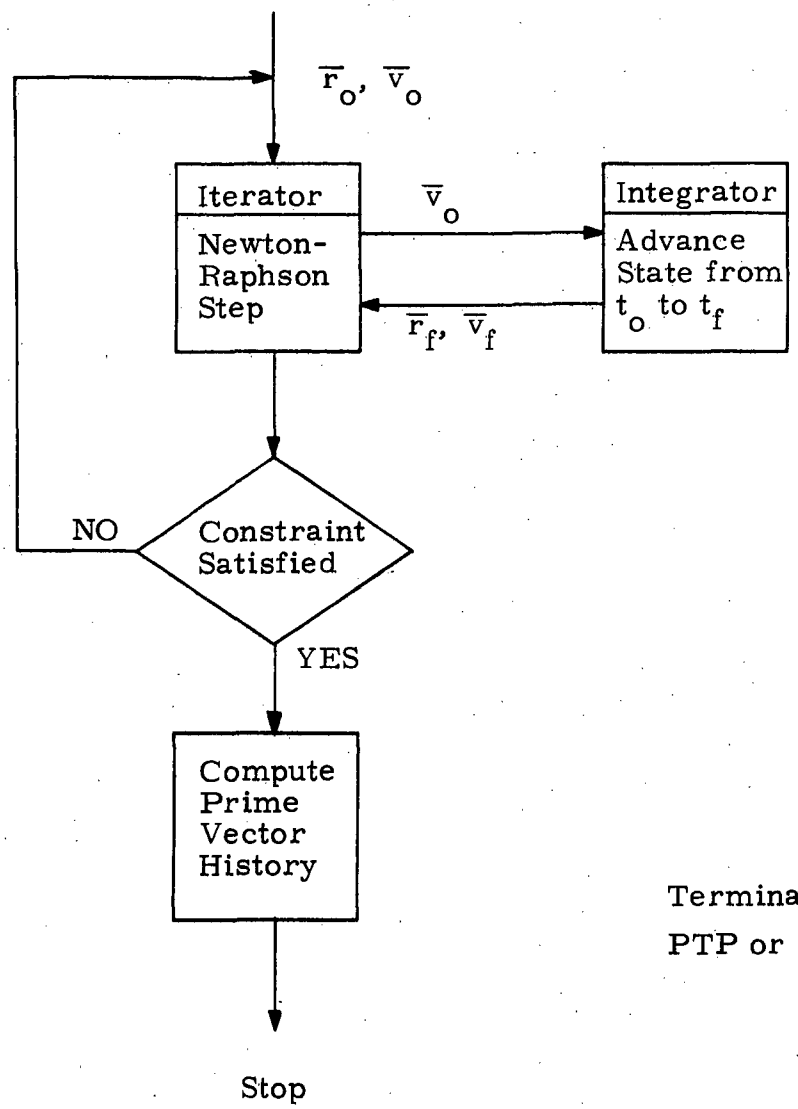

Figure 14 TWO-IMPULSE TRANSFER WITHOUT OPTIMIZATION

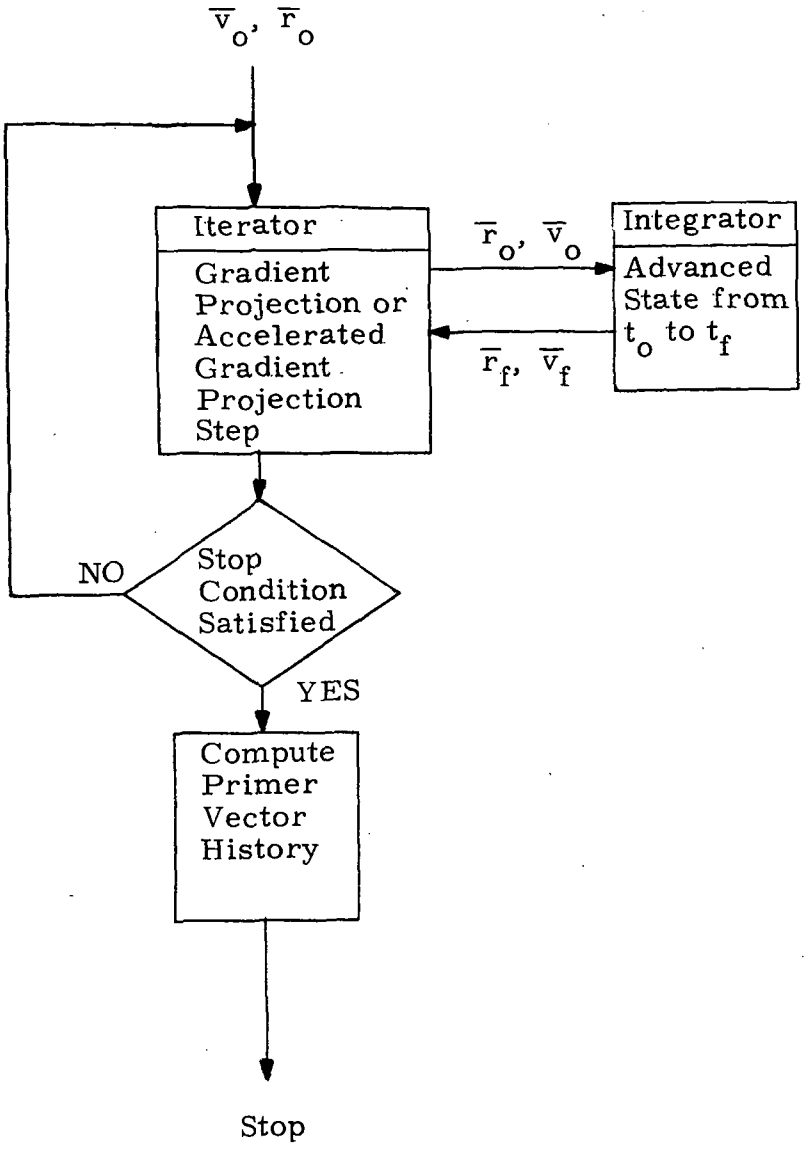

Figure 15 TWO-IMPULSE TRANSFER WITH OPTIMIZATION

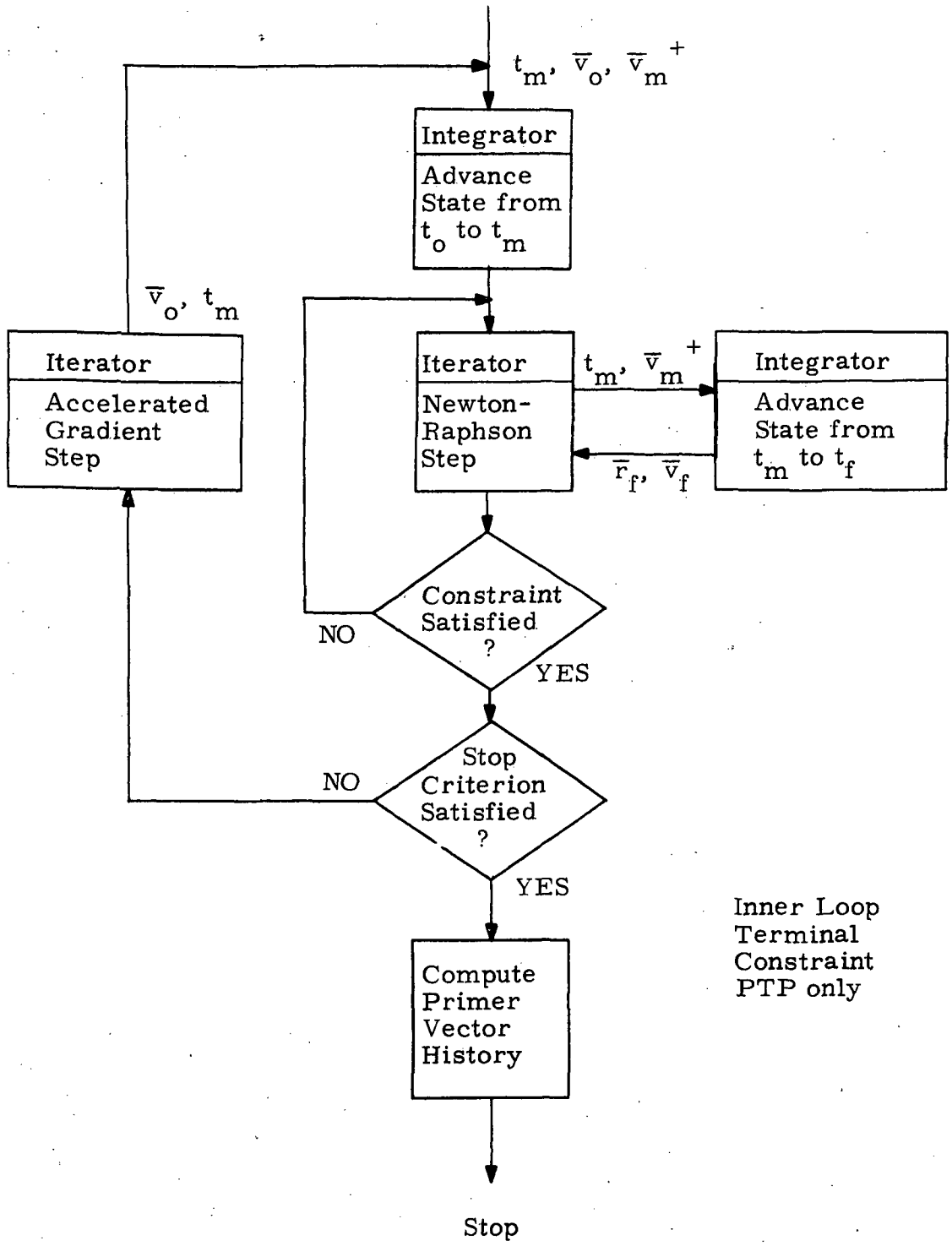

Figure 16 THREE-IMPULSE TRANSFER

problem to be solved. Tests have shown that it is possible to reduce computer time by 50%.

The proposed program structures for 2- and 3-impulse transfers are shown in Figs. 14, 15 and 16.

II.4.1 Two-Impulse Transfer from Earth to a Point in Space

It is assumed that the initial position of the vehicle lies on a circular earth parking orbit of known radius r_o and is specified by two angles, α and β. (Fig. 17) The initial required velocity is assumed to be normal to the position vector and makes an angle γ with an intermediate plane. The $X_E Y_E Z_E$ coordinates are inertial non-rotating coordinates. The three angles and the magnitude of the required velocity, v_o, are to be chosen so that the cost of transfer from the earth to a specified point (P) in a specified time is optimized (Fig. 18).

II.4.1.1 Estimate of Initial Required Velocity at Earth

An estimate of the initial required velocity at earth for a 2-impulse transfer to a point in space may be generated as follows. Let

$\bar{r}_{EV}$ = position vector in $X_E Y_E Z_E$ coordinates

r_o = magnitude of position vector

Rotation matrices (from $X'Y'Z'$ to $X_E Y_E Z_E$):

$$R_\alpha = \begin{pmatrix} \cos\alpha & -\sin\alpha & 0 \\ \sin\alpha & \cos\alpha & 0 \\ 0 & 0 & 1 \end{pmatrix}$$

$$R_\beta = \begin{pmatrix} \cos\beta & 0 & -\sin\beta \\ 0 & 1 & 0 \\ \sin\beta & 0 & \cos\beta \end{pmatrix}$$

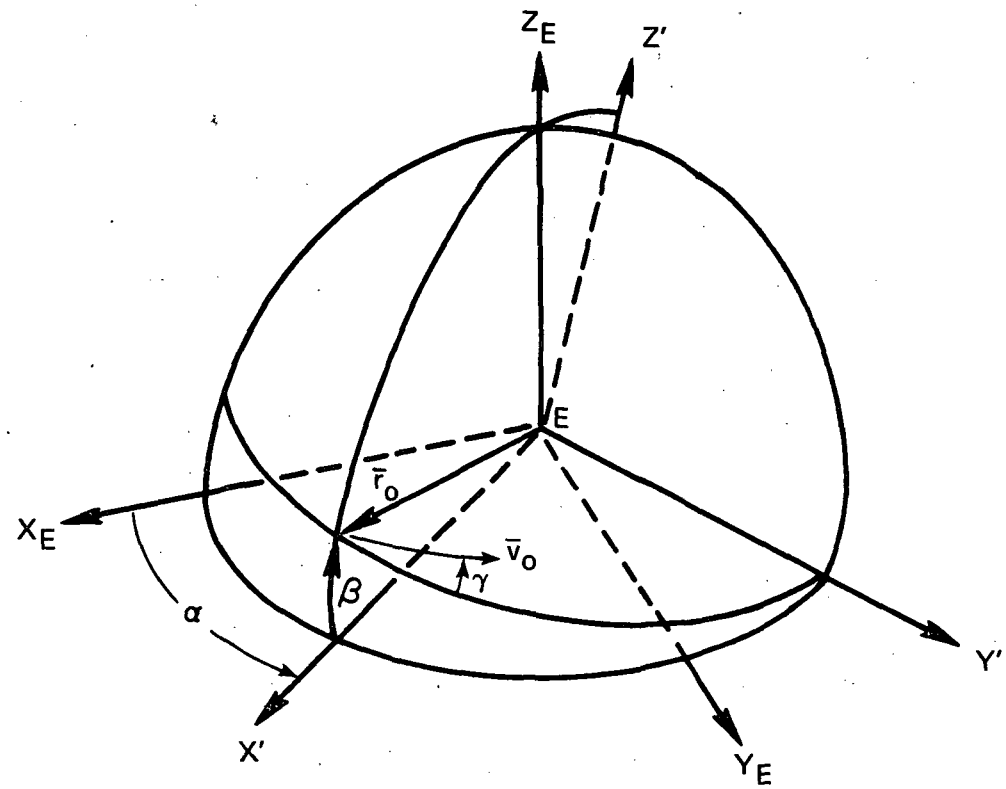

Fig. 17. Initial position and velocity vectors of a 2 - impulse transfer from earth.

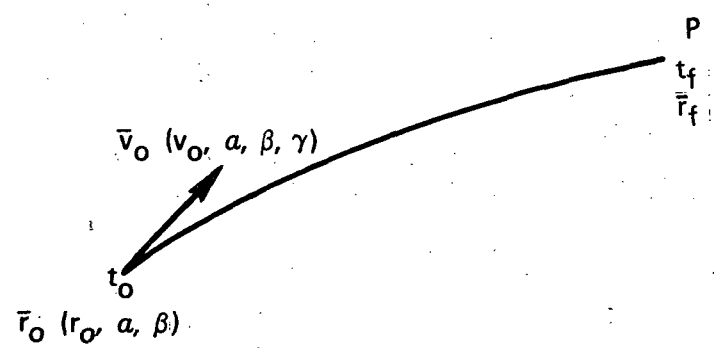

Fig. 18. Two - impulse transfer from earth to P.

$$R_\gamma = \begin{pmatrix} 1 & 0 & 0 \\ 0 & \cos\gamma & -\sin\gamma \\ 0 & \sin\gamma & \cos\gamma \end{pmatrix}$$

Then

$$\bar{r}_{EV} = R_\alpha R_\beta \begin{pmatrix} r_o \\ 0 \\ 0 \end{pmatrix}$$

$$= \begin{pmatrix} r_o & \cos\alpha & \cos\beta \\ r_o & \sin\alpha & \cos\beta \\ r_o & \sin\beta & \end{pmatrix}$$

$$\bar{v}_{EV} = R_\alpha R_\beta R_\gamma \begin{pmatrix} 0 \\ v_o \\ 0 \end{pmatrix}$$

$$= \begin{pmatrix} v_o & (-\sin\alpha\cos\gamma - \cos\alpha\sin\beta\sin\gamma) \\ v_o & (\cos\alpha\cos\gamma - \sin\alpha\sin\beta\sin\gamma) \\ v_o & \cos\beta\sin\gamma \end{pmatrix}$$

$$\bar{r}_o = \bar{r}_{SV} = \bar{r}_{SE} + \bar{r}_{EV}$$

$$\bar{v}_o = \bar{v}_{SV} = \bar{v}_{SE} + \bar{v}_{EV}$$

where $\bar{r}_o$ and $\bar{v}_o$ are position and velocity vectors relative to the sun in X-Y-Z coordinates.

For a specified transfer time and magnitude of the initial impulse the initial required velocity is expressed in terms of the 3 angles. By varying α, β and γ in small increments a field of trajectories is generated. A crude search is made first for the required velocity which gives the minimum miss distance. This is followed by a refined search around

the above minimum.

II. 4. 1. 2 Cost and Constraint Gradients

Independent variables:

$$\overline{x} = (v_o, \alpha, \beta, \gamma)$$

State transition matrix:

$$\varphi(t_f, t_o) = \begin{pmatrix} \varphi_{11} & \varphi_{12} \\ \varphi_{21} & \varphi_{22} \end{pmatrix}$$

Terminal condition:

$$\overline{\psi} = \overline{r}_f - \overline{r}_{fd}$$

Variational equations:

$$\delta\overline{r}_f = \varphi_{11}\, \delta\overline{r}_o + \varphi_{12}\, \delta\overline{v}_o$$

$$\delta\overline{v}_f = \varphi_{21}\, \delta\overline{r}_o + \varphi_{22}\, \delta\overline{v}_o$$

The variations of the initial position and velocity are related to the changes in the independent variables by

$$\delta\overline{r}_o = \frac{\partial\overline{r}_o}{\partial\overline{x}}\, d\overline{x}$$

$$\delta\overline{v}_o = \frac{\partial\overline{v}_o}{\partial\overline{x}}\, d\overline{x}$$

$$\delta\overline{r}_f = \left[\varphi_{11} \frac{\partial\overline{r}_o}{\partial\overline{x}} + \varphi_{12} \frac{\partial\overline{v}_o}{\partial\overline{x}}\right] d\overline{x} = \frac{\partial\overline{r}_f}{\partial\overline{x}}\, d\overline{x}$$

$$\delta\bar{v}_f = \left[\varphi_{21}\frac{\partial\bar{r}_o}{\partial\bar{x}} + \varphi_{22}\frac{\partial\bar{v}_o}{\partial\bar{x}}\right] d\bar{x} = \frac{\partial\bar{v}_f}{\partial\bar{x}}\, d\bar{x}$$

$$\frac{\partial\bar{r}_o}{\partial\bar{x}} = \left[\begin{array}{c|c|c|c} 0 & -r_o \sin\alpha\cos\beta & -r_o\cos\alpha\sin\beta & 0 \\ 0 & r_o\cos\alpha\cos\beta & -r_o\sin\alpha\sin\beta & 0 \\ 0 & 0 & r_o\cos\beta & 0 \end{array}\right]$$

$$\frac{\partial\bar{v}_o}{\partial\bar{x}} = \left[\begin{array}{c|c|c|c} -\sin\alpha\cos\gamma - \cos\alpha\sin\beta\sin\gamma & v_o(-\cos\alpha\cos\gamma + \sin\alpha\sin\beta\sin\gamma) & -v_o\cos\alpha\cos\beta\sin\gamma & v_o(\sin\alpha\sin\gamma - \cos\alpha\sin\beta\cos\gamma) \\ \cos\alpha\cos\gamma - \sin\alpha\sin\beta\sin\gamma & vo(-\sin\alpha\cos\gamma - \cos\alpha\sin\beta\sin\gamma) & -v_o\sin\alpha\cos\beta\sin\gamma & v_o(-\cos\alpha\sin\gamma - \sin\alpha\sin\beta\cos\gamma) \\ \cos\beta\sin\gamma & 0 & -v_o\sin\beta\sin\gamma & v_o\cos\beta\cos\gamma \end{array}\right]$$

Cost gradient:

$$\Delta v = |\bar{v}_{fd} - \bar{v}_f|$$

$$= |\Delta\bar{v}_f|$$

$$\frac{\partial|\Delta\bar{v}_f|}{d\bar{x}} = \frac{-\Delta\bar{v}_f^{\,T}}{|\Delta\bar{v}_f|}\frac{\partial\bar{v}_f}{\partial\bar{x}} = \frac{-\Delta\bar{v}_f^{\,T}}{|\Delta\bar{v}_f|}\left[\varphi_{21}\frac{\partial\bar{r}_o}{\partial\bar{x}} + \varphi_{22}\frac{\partial\bar{v}_o}{\partial\bar{x}}\right]$$

$$\frac{\partial\Delta v}{\partial\bar{x}} = \frac{\partial|\Delta\bar{v}_f|}{\partial\bar{x}}$$

Note that only the Δv at the terminal point is considered.

Constraint gradient:

$$\frac{\partial \overline{\psi}}{\partial \overline{x}} = \frac{\partial}{\partial \overline{x}} (\overline{r}_f - \overline{r}_{fd}) = \frac{\partial \overline{r}_f}{\partial \overline{x}} = \varphi_{11} \frac{\partial \overline{r}_o}{\partial \overline{x}} + \varphi_{12} \frac{\partial \overline{v}_o}{\partial \overline{x}}$$

II.4.2 Two-Impulse Transfer from a Point in Space to Earth

The 2-impulse transfer from a point in space to the earth is shown in Fig. 19. An estimate of the initial velocity may be generated in a manner similar to the transfer from the earth to a point in space.

Independent variables:

$$\overline{x} = \overline{v}_o$$

State Transition matrix:

$$\varphi(t_f, t_o) = \begin{pmatrix} \varphi_{11} & \varphi_{12} \\ \varphi_{21} & \varphi_{22} \end{pmatrix}$$

Variational equations:

$$\delta \overline{r}_f = \varphi_{12} \, \delta \overline{v}_o$$

$$\delta \overline{v}_f = \varphi_{22} \, \delta \overline{v}_o$$

It follows,

$$\frac{\partial \overline{r}_f}{\partial \overline{v}_o} = \varphi_{12}$$

$$\frac{\partial \overline{v}_f}{\partial \overline{v}_o} = \varphi_{22}$$

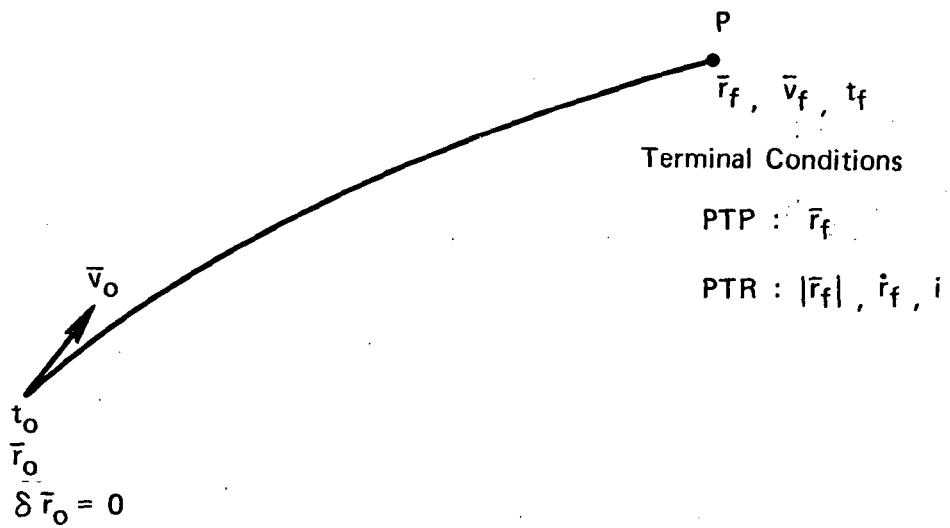

Fig. 19. 2 - Impulse Transfer from a Point in Space to Earth.

Cost gradient:

$$\Delta v = |\Delta \bar{v}_o| + |\Delta \bar{v}_f| = |\bar{v}_o - \bar{v}_o^-| + |\bar{v}_{fd} - \bar{v}_f|$$

where

$$\bar{v}_{fd} = \sqrt{\frac{\mu_E}{r_{fE}}}\ \text{unit}\ ((\bar{r}_f \times \bar{v}_f) \times \bar{r}_f)_{\text{Earth}} + \bar{v}_{SE}$$

$\bar{v}_{SE}$ = velocity to earth

r_{fE} = radial distance of vehicle at earth

$$\frac{\partial \Delta v}{\partial \bar{v}_o} = \frac{\Delta \bar{v}_o^T}{|\Delta \bar{v}_o|} - \frac{\Delta \bar{v}_f^T}{|\Delta \bar{v}_f|} \frac{\partial \bar{v}_f}{\partial \bar{v}_o}$$

$$= \frac{\Delta \bar{v}_o^T}{|\Delta \bar{v}_o|} - \frac{\Delta \bar{v}_f^T}{|\Delta \bar{v}_f|} \varphi_{22}$$

Point to Radius Terminal Condition (PTR)

$$\bar{\psi}(t_f) = \begin{pmatrix} r_{fd} & - & r_f \\ \dot{r}_{fd} & - & \dot{r}_f \\ \cos i_d & - & \cos i \end{pmatrix}_{\text{Earth}}$$

where

$$r_f = |\bar{r}_f|$$

$$\dot{r}_f = \bar{r}_f^T \bar{v}_f / r_f$$

$$\cos i = \bar{u}_Z^T \bar{h}/h$$

$$\bar{h} = \bar{r}_f \times \bar{v}_f$$

$$\bar{u}_Z = (0,\ 0,\ 1)$$

$$\frac{\partial \overline{\psi}}{\partial \overline{v}_o} = -\begin{pmatrix} \dfrac{\partial r_f}{\partial \overline{v}_o} \\ \dfrac{\partial \dot{r}_f}{\partial \overline{v}_o} \\ \dfrac{\partial \cos i}{\partial \overline{v}_o} \end{pmatrix}$$

$$\frac{\partial r_f}{\partial \overline{v}_o} = \frac{\overline{r}_f^{\,T}}{r_f} \frac{\partial \overline{r}_f}{\partial \overline{v}_o} = \frac{1}{r_f} \overline{r}_f^{\,T} \varphi_{12}$$

$$\frac{\partial \dot{r}_f}{\partial \overline{v}_o} = \frac{1}{r_f^2} \left[(r_f \overline{v}_f^{\,T} - \dot{r}_f \overline{r}_f^{\,T}) \varphi_{12} + r_f \overline{r}_f^{\,T} \varphi_{22} \right]$$

$$\frac{\partial \cos i}{\partial \overline{v}_o} = \overline{u}_Z^{\,T} \frac{\partial (\overline{h}/h)}{\partial \overline{v}_o}$$

$$= \overline{u}_Z^{\,T} \left[\frac{1}{h} \frac{\partial \overline{h}}{\partial \overline{v}_o} - \frac{\overline{h}}{h^2} \frac{\partial h}{\partial \overline{v}_o} \right]$$

Define:

$$R = \begin{pmatrix} 0 & -z_f & y_f \\ z_f & 0 & -x_f \\ -y_f & x_f & 0 \end{pmatrix}$$

$$V = \begin{pmatrix} 0 & -\dot{z}_f & \dot{y}_f \\ \dot{z}_f & 0 & -\dot{x}_f \\ -\dot{y}_f & \dot{x}_f & 0 \end{pmatrix}$$

then,

$$\frac{\partial \bar{h}}{\partial \bar{v}_o} = \bar{r}_f \times \frac{\partial \bar{v}_f}{\partial \bar{v}_o} - \bar{v}_f \times \frac{\partial \bar{r}_f}{\partial \bar{v}_o}$$

$$= R\,\varphi_{22} - V\,\varphi_{12}$$

$$\frac{\partial h}{\partial \bar{v}_o} = \frac{\bar{h}^T}{h} \frac{\partial \bar{h}}{\partial \bar{v}_o}$$

$$= \frac{\bar{h}^T}{h} (R\,\varphi_{22} - V\,\varphi_{12})$$

$$\frac{\partial \cos i}{\partial \bar{v}_o} = \frac{\bar{u}_z^T}{h^3} (h^2 I - \bar{h}\bar{h}^T) (R\,\varphi_{22} - V\,\varphi_{12})$$

Point to Point Terminal Condition (PTP)

$$\bar{\psi}(t_f) = \bar{r}_f - \bar{r}_{fd}$$

$$\frac{\partial \bar{\psi}}{\partial \bar{v}_o} = \frac{\partial \bar{r}_f}{\partial \bar{v}_o} = \varphi_{12}$$

II.4.3 Three-Impulse Transfer[2, 3]

A 3-impulse transfer between 2 points in space is shown in Fig. 20. Given a reference trajectory Γ, the problem is to generate a neighboring trajectory Γ' satisfying the same boundary conditions at reduced ΔV.

II.4.3.1 Classical Three-Impulse Transfer

In the classical approach, there is an outer loop which iterates on $\bar{r}_m$ and t_m to reduce ΔV and two inner loops which iterate on $\bar{v}_o$ and $\bar{v}_m^+$ to satisfy boundary conditions at t_m and t_f respectively. The cost gradient of the outer loop is expressed in terms of the primer vector and its time derivatives.

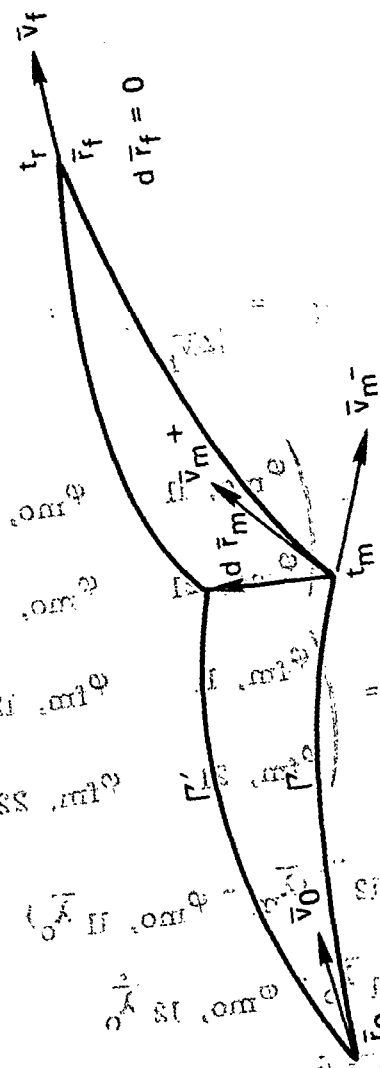

Fig. 20. 3 - Impulse Transfer.

$$\Delta v = |\bar{v}_o - \bar{v}_o^-| + |\bar{v}_m^+ - \bar{v}_m^-| + |\bar{v}_{fd} - \bar{v}_f|$$

$$= |\Delta\bar{v}_o| + |\Delta\bar{v}_m| + |\Delta\bar{v}_f|$$

$$\bar{\lambda}_o = \frac{\Delta\bar{v}_o}{|\Delta\bar{v}_o|}$$

$$\bar{\lambda}_m = \frac{\Delta\bar{v}_m}{|\Delta\bar{v}_m|}$$

$$\bar{\lambda}_f = \frac{\Delta\bar{v}_f}{|\Delta\bar{v}_f|}$$

$$\varphi_{mo}(t_m, t_o) = \begin{pmatrix} \varphi_{mo,\,11} & \varphi_{mo,\,12} \\ \varphi_{mo,\,21} & \varphi_{mo,\,22} \end{pmatrix}$$

$$\varphi_{fm}(t_f, t_m) = \begin{pmatrix} \varphi_{fm,\,11} & \varphi_{fm,\,12} \\ \varphi_{fm,\,21} & \varphi_{fm,\,22} \end{pmatrix}$$

$$\dot{\bar{\lambda}}_o = \varphi_{mo,\,12}^{-1}(\bar{\lambda}_m - \varphi_{mo,\,11}\,\bar{\lambda}_o)$$

$$\dot{\bar{\lambda}}_m^- = \varphi_{mo,\,11}\,\bar{\lambda}_o + \varphi_{mo,\,12}\,\dot{\bar{\lambda}}_o$$

$$\dot{\bar{\lambda}}_m^+ = \varphi_{fm,\,12}^{-1}(\bar{\lambda}_f - \varphi_{fm,\,11}\,\bar{\lambda}_m)$$

Cost gradient:

$$\frac{\partial \Delta v}{\partial \bar{r}_m} = (\dot{\bar{\lambda}}_m^+ - \dot{\bar{\lambda}}_m^-)^T$$

$$\frac{\partial \Delta v}{\partial t_m} = -(\dot{\bar{\lambda}}_m^{+} \cdot \bar{v}_m^{+} - \dot{\bar{\lambda}}_m^{-} \cdot \bar{v}_m^{-})$$

II.4.3.2 New Three-Impulse Transfer

The independent variables in the outer loop are changed to $\bar{v}_o$ and t_m. The state vector is extrapolated to t_m. There is only one inner loop which iterates on $\bar{v}_m^{+}$ to satisfy terminal condition $\bar{r}_{fd}$.

Cost and Cost Gradient

$$\Delta v = |\Delta \bar{v}_o| + |\Delta \bar{v}_m| + |\Delta \bar{v}_f|$$

$$= |\bar{v}_o - \bar{v}_o^{-}| + |\bar{v}_m^{+} - \bar{v}_m^{-}| + |\bar{v}_{fd} - \bar{v}_f|$$

$$\frac{\partial \Delta v}{\partial \bar{v}_o} = \frac{\Delta \bar{v}_o}{|\Delta \bar{v}_o|} + \frac{\Delta \bar{v}_m}{|\Delta \bar{v}_m|}\left(\frac{\partial \bar{v}_m^{+}}{\partial \bar{v}_o} - \frac{\partial \bar{v}_m^{-}}{\partial \bar{v}_o}\right) - \frac{\Delta \bar{v}_f}{|\Delta \bar{v}_f|}\frac{\partial \bar{v}_f}{\partial \bar{v}_o}$$

$$= \bar{\lambda}_o^{T} + \bar{\lambda}_m^{T}\left(\frac{\partial \bar{v}_m^{+}}{\partial \bar{v}_o} - \frac{\partial \bar{v}_m^{-}}{\partial \bar{v}_o}\right) - \bar{\lambda}_f^{T}\frac{\partial \bar{v}_f}{\partial \bar{v}_o}$$

$$\frac{\partial \Delta v}{\partial t_m} = \bar{\lambda}_m^{T}\left(\frac{\partial \bar{v}_m^{+}}{\partial t_m} - \frac{\partial \bar{v}_m^{-}}{\partial t_m}\right) - \bar{\lambda}_f^{T}\frac{\partial \bar{v}_f}{\partial t_m}$$

Variational Equations for the first leg

$$\delta \bar{r}_m^{-} = \varphi_{mo,\,11}\,\delta \bar{r}_o + \varphi_{mo,\,12}\,\delta \bar{v}_o = \varphi_{mo,\,12}\,\delta \bar{v}_o$$

$$\delta \bar{v}_m^{-} = \varphi_{mo,\,21}\,\delta \bar{r}_o + \varphi_{mo,\,22}\,\delta \bar{v}_o = \varphi_{mo,\,22}\,\delta \bar{v}_o$$

$$\delta \bar{r}_o = 0$$

$$\frac{\delta \bar{r}_m^-}{\partial \bar{v}_o} = \varphi_{mo,\ 12}$$

$$\frac{\partial \bar{v}_m^-}{\partial \bar{v}_o} = \varphi_{mo,\ 22}$$

$$\frac{\partial \bar{v}_m^-}{\partial t_m} = 0$$

Variational Equations for the second leg

$$\delta \bar{r}_f = 0 = \varphi_{fm,\ 11}\, \delta \bar{r}_m^+ + \varphi_{fm,\ 12}\, \delta \bar{v}_m^+$$

$$\delta \bar{v}_f = \varphi_{fm,\ 21}\, \delta \bar{r}_m^+ + \varphi_{fm,\ 22}\, \delta \bar{v}_m^+$$

$$\therefore \quad \delta \bar{v}_m^+ = -\varphi_{fm,\ 12}\, \varphi_{fm,\ 11}\, \delta \bar{r}_m^+$$

Since

$$d\bar{r}_m = \delta \bar{r}_m^- + \bar{v}_m^-\, dt_m = \delta \bar{r}_m^+ + \bar{v}_m^+\, dt_m$$

$$\delta \bar{r}_m^+ = \delta \bar{r}_m^- - (\bar{v}_m^+ - \bar{v}_m^-)\, dt_m$$

$$\therefore \quad \delta \bar{v}_m^+ = -\varphi_{fm,\ 12}^{-1}\, \varphi_{fm,\ 11}\, [\delta \bar{r}_m^- - (\bar{v}_m^+ - \bar{v}_m^-)\, dt_m]$$

$$= -\varphi_{fm,12}^{-1}\, \varphi_{fm,11}\, \varphi_{mo,12}\, \delta \bar{v}_o + \varphi_{fm,12}^{-1}\, \varphi_{fm,11}\, (\bar{v}_m^+ - \bar{v}_m^-)\, dt_m$$

$$\frac{\partial \bar{v}_m^+}{\partial \bar{v}_o} = -\varphi_{fm,\,12}^{-1}\,\varphi_{fm,\,11}\,\varphi_{mo,\,12}$$

$$\frac{\partial \bar{v}_m^+}{\partial t_m} = \varphi_{fm,\,12}^{-1}\,\varphi_{fm,\,11}\,(\bar{v}_m^+ - \bar{v}_m^-)$$

$$\delta\bar{v}_f = \varphi_{fm,\,21}\,[\delta\bar{r}_m^- - (\bar{v}_m^+ - \bar{v}_m^-)\,dt_m]$$

$$+ \varphi_{fm,22}\,[-\varphi_{fm,12}^{-1}\,\varphi_{fm,11}\,\varphi_{mo,12}\,\delta\bar{v}_o + \varphi_{fm,12}^{-1}\,\varphi_{fm,11}\,(\bar{v}_m^+ - \bar{v}_m^-)\,dt_m]$$

$$= [\varphi_{fm,\,21} - \varphi_{fm,22}\,\varphi_{fm,12}^{-1}\,\varphi_{fm,11}]\,\varphi_{mo,\,12}\,\delta\bar{v}_o$$

$$+ [-\varphi_{fm,21} + \varphi_{fm,22}\,\varphi_{fm,12}^{-1}\,\varphi_{fm,11}]\,(\bar{v}_m^+ - \bar{v}_m^-)\,dt_m$$

$$\frac{\partial \bar{v}_f}{\partial \bar{v}_o} = [\varphi_{fm,\,21} - \varphi_{fm,\,22}\,\varphi_{fm,\,12}^{-1}\,\varphi_{fm,\,11}]\,\varphi_{mo,\,12}$$

$$\frac{\partial \bar{v}_f}{\partial t_m} = -[\varphi_{fm,\,21} - \varphi_{fm,\,22}\,\varphi_{fm,\,12}^{-1}\,\varphi_{fm,\,11}]\,(\bar{v}_m^+ - \bar{v}_m^-)\,dt_m$$

Note: This derivation does not need the computation of the primer vector and its derivative.

II. 4. 3. 3 An Alternate Form of Cost Gradient from Classical Approach

In Classical Approach[2, 3]

$$\text{on } \Gamma: \quad J = |\Delta\bar{v}_o| + |\Delta\bar{v}_m| + |\Delta\bar{v}_f|$$

on Γ': $J' = |\Delta\bar{v}_o + \delta\bar{v}_o| + |\Delta\bar{v}_m + \delta\bar{v}_m^+ - \delta\bar{v}_m^-| + |\Delta\bar{v}_f + \delta\bar{v}_f|$

$$\delta J = J' - J = \bar{\lambda}_o^T \delta\bar{v}_o + \bar{\lambda}_m^T (\delta\bar{v}_m^+ - \delta\bar{v}_m^-) - \bar{\lambda}_f^T \delta\bar{v}_f$$

Applying the relation

$$\bar{\lambda}^T \delta\bar{v} - \dot{\bar{\lambda}}^T \delta\bar{x} = C$$

between impulses, we have

$$\bar{\lambda}_o^T \delta\bar{v}_o - \dot{\bar{\lambda}}_o^T \delta\bar{r}_o = \bar{\lambda}_o^T \delta\bar{v}_o = \bar{\lambda}_m^{T-} \delta\bar{v}_m^- - \dot{\bar{\lambda}}_m^{T-} \delta\bar{r}_m^-$$

$$\bar{\lambda}_o^T \delta\bar{v}_f - \dot{\bar{\lambda}}_f^T \delta\bar{r}_f = \bar{\lambda}_f^T \delta\bar{v}_f = \bar{\lambda}_m^{T+} \delta\bar{v}_m^+ - \dot{\bar{\lambda}}_m^{T+} \delta\bar{r}_m^+$$

Since

$$\bar{\lambda}_m^+ = \bar{\lambda}_m^- = \bar{\lambda}_m,$$

$$\bar{\lambda}_o^T \delta\bar{v}_o - \bar{\lambda}_f^T \delta\bar{v}_f = -\bar{\lambda}_m^T (\delta\bar{v}_m^+ - \delta\bar{v}_m^-) + (\dot{\bar{\lambda}}_m^{T+} \delta\bar{r}_m^+ - \dot{\bar{\lambda}}_m^{T-} \delta\bar{r}_m^-)$$

$$\delta J = \dot{\bar{\lambda}}_m^{T+} \delta\bar{r}_m^+ - \dot{\bar{\lambda}}_m^{T-} \delta\bar{r}_m^-$$

$$= \dot{\bar{\lambda}}_m^{T+} (d\bar{r}_m - \bar{v}_m^+ dt_m) - \dot{\bar{\lambda}}_m^{T-} (d\bar{r}_m - \bar{v}_m^- dt_m)$$

$$= (\dot{\bar{\lambda}}_m^+ - \dot{\bar{\lambda}}_m^-)^T d\bar{r}_m - (\dot{\bar{\lambda}}_m^{T+} \bar{v}_m^+ - \dot{\bar{\lambda}}_m^{T-} \bar{v}_m^-) dt_m$$

$\bar{r}_m$, t_m = independent variables used by Lion and Handelsman and Jezewski.

If we use the relation

$$-\dot{\bar{\lambda}}_m^{T-}\,\delta\bar{r}_m^{-} = \bar{\lambda}_o^{T}\,\delta\bar{v}_o - \bar{\lambda}_m^{T-}\,\delta\bar{v}_m^{-}$$

$$\dot{\bar{\lambda}}_m^{T+}\,\delta\bar{r}_m^{+} = -\bar{\lambda}_f^{T}\,\delta\bar{v}_f + \bar{\lambda}_m^{T+}\,\delta\bar{v}_m^{+}$$

we return to

$$\delta J = \bar{\lambda}_o^{T}\,\delta\bar{v}_o + \bar{\lambda}_m^{T}\,(\delta\bar{v}_m^{+} - \delta\bar{v}_m^{-}) - \bar{\lambda}_f^{T}\,\delta\bar{v}_f$$

which will lead to same gradient as before. However, if we use the expressions for $\dot{\lambda}_m^{+}$ and $\dot{\lambda}_m^{-}$ in

$$\delta J = \dot{\bar{\lambda}}_m^{+}\,\delta\bar{r}_m^{+} - \dot{\bar{\lambda}}_m^{T-}\,\delta\bar{r}_m^{-}$$

we will get a different but equivalent expression for the gradient. This is because of $\bar{\lambda}_o$ and $\bar{\lambda}_f$ are related through the relation

$$\bar{\lambda}^{T}\,\delta v - \dot{\bar{\lambda}}^{T}\,\delta\bar{x} = C.$$

Since

$$\bar{\lambda}_m = \varphi_{mo,\,11}\,\bar{\lambda}_o + \varphi_{mo,\,12}\,\dot{\bar{\lambda}}_o$$

$$\dot{\bar{\lambda}}_m^{-} = \varphi_{mo,\,21}\,\bar{\lambda}_o + \varphi_{mo,\,22}\,\dot{\bar{\lambda}}_o$$

we have

$$\dot{\bar{\lambda}}_o = \varphi_{mo,\,12}^{-1}\,(\bar{\lambda}_m - \varphi_{mo,\,11}\,\bar{\lambda}_o)$$

$$\dot{\bar{\lambda}}_m^{-} = \varphi_{mo,\,21}\,\bar{\lambda}_o + \varphi_{mo,\,22}\,\varphi_{mo,\,12}^{-1}\,(\bar{\lambda}_m - \varphi_{mo,\,11}\,\bar{\lambda}_o)$$

Similarly,

$$\bar{\lambda}_f = \varphi_{fm,\,11}\,\bar{\lambda}_m + \varphi_{fm,\,12}\,\dot{\bar{\lambda}}_m^{+}$$

$$\dot{\bar{\lambda}}_f = \varphi_{fm,\,21}\,\bar{\lambda}_m + \varphi_{fm,\,22}\,\dot{\bar{\lambda}}_m^{+}$$

$$\therefore \quad \dot{\bar{\lambda}}_m^{+} = \varphi_{fm,\,12}^{-1}\,(\bar{\lambda}_f - \varphi_{fm,\,11}\,\bar{\lambda}_m)$$

$$\delta J = \dot{\bar{\lambda}}_m^{T+}\,\delta\bar{r}_m^{+} - \dot{\bar{\lambda}}_m^{T-}\,\delta\bar{r}_m^{-}$$

$$= \dot{\bar{\lambda}}_m^{T+}\,[\delta\bar{r}_m^{-} - (\bar{v}_m^{+} - \bar{v}_m^{-})\,dt_m] - \dot{\bar{\lambda}}_m^{T-}\,\delta\bar{r}_m^{-}$$

$$= (\dot{\bar{\lambda}}_m^{T+} - \dot{\bar{\lambda}}_m^{T-})\,\delta\bar{r}_m^{-} - \dot{\bar{\lambda}}_m^{T+}\,(\bar{v}_m^{+} - \bar{v}_m^{-})\,dt_m$$

$$= [\varphi_{fm,\,12}^{-1}\,(\bar{\lambda}_f - \varphi_{fm,\,11}\,\bar{\lambda}_m)$$

$$- \varphi_{mo,\,21}\,\bar{\lambda}_o - \varphi_{mo,\,22}\,\varphi_{mo,\,12}^{-1}\,(\bar{\lambda}_m - \varphi_{mo,\,11}\,\bar{\lambda}_o)]^T\,\delta\bar{r}_m^{-}$$

$$- [\varphi_{fm,\,12}^{-1}\,(\bar{\lambda}_f - \varphi_{fm,11}\,\bar{\lambda}_m)]^T\,(\bar{v}_m^{+} - \bar{v}_m^{-})\,dt_m$$

$$= \{[-\varphi_{mo,\,21} + \varphi_{mo,\,22}\,\varphi_{mo,\,12}^{-1}\,\varphi_{mo,\,11}]\,\bar{\lambda}_o$$

$$+ [-\varphi_{fm,\,12}^{-1}\,\varphi_{fm,\,11} - \varphi_{mo,\,22}\,\varphi_{mo,\,12}^{-1}]\,\bar{\lambda}_m$$

$$+ \varphi_{fm,\,12}^{-1}\,\bar{\lambda}_f\}^T\,\varphi_{mo,\,12}\,\delta\bar{v}_o$$

$$+ [\varphi_{fm,\,12}^{-1}\,(\varphi_{fm,\,11}\,\bar{\lambda}_m - \bar{\lambda}_f)]^T\,(\bar{v}_m^{+} - \bar{v}_m^{-})\,dt_m$$

Thus

$$\frac{\partial\Delta^v}{\partial\bar{v}_o} = \{[-\varphi_{mo,\,21} + \varphi_{mo,\,22}\,\varphi_{mo,\,12}^{-1}\,\varphi_{mo,\,11}]\,\bar{\lambda}_o$$

$$- [\varphi_{fm,\,12}^{-1}\,\varphi_{fm,\,11} + \varphi_{mo,\,22}\,\varphi_{mo,\,12}^{-1}]\,\bar{\lambda}_m$$

$$+ \varphi_{fm,\,12}^{-1}\,\bar{\lambda}_f\}^T\,\varphi_{mo,\,12}$$

$$\frac{\partial \Delta v}{\partial t_m} = [\varphi_{fm,\ 12}^{-1} (\varphi_{fm,\ 11} \bar{\lambda}_m - \bar{\lambda}_f)]^T (\bar{v}_m^+ - \bar{v}_m^-)\, dt_m$$

These cost gradients are different in appearance from the previous result.

The constraint gradient with respect to the required velocity in the inner loop of the three-impulse case is the same as shown in the two-impulse transfer from a point to earth by iterating on $\bar{v}_m^+$ instead of $\bar{v}_o$.

II.4.3.4 Solution of Inner Loop Lambert Problem in Increments

The change in the interior impulse position, $d\bar{r}_m$, between the perturbed and reference trajectories due to changes in $\bar{v}_o$ and t_m is usually so large that the $\bar{v}_m^+$ on the reference trajectory is a poor estimate for the inner loop Lambert problem. This difficulty can be alleviated by introducing $d\bar{r}_m$ in increments rather than in one step. (Fig. 21).

Using $\bar{v}_o$, t_m from the outer loop, we extrapolate the state vector to t_m to obtain $\bar{r}_m$.

$$d\bar{r}_m = \bar{r}_m - \bar{r}_{m,\ old}$$

Let n = number of increments

$$\Delta\bar{r}_m = \frac{d\bar{r}_m}{n}$$

$$j = 0$$

Procedure:

1. $$\bar{r}_{m,\ new} = \bar{r}_{m,\ old} + \Delta\bar{r}_m$$

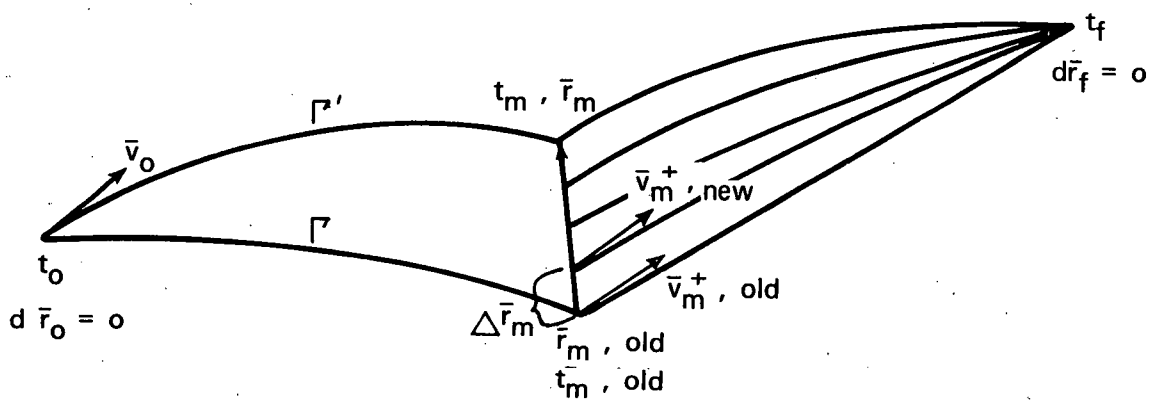

Fig. 21. Solution of Inner Loop Lambert Problem in Increments.

2. $$\Delta\bar{v}_m^{+} = -\varphi_{fm,\,12}^{-1}\,\varphi_{fm,\,11}\,\Delta\bar{r}_m$$

$$\bar{v}_{m,\,new}^{+} = \bar{v}_{m,\,old}^{+} + \Delta\bar{v}_m^{+}$$

3. Solve inner loop Lambert problem from $\bar{r}_{m,\,new}$ to $\bar{r}_{fd}$ using $\bar{v}_{m,\,new}^{+}$ as the initial estimate.

4. $$\bar{v}_{m,\,old}^{+} = \bar{v}_{m,\,new}^{+}$$

$$\bar{r}_{m,\,old} = \bar{r}_{m,\,new}$$

$$j = j + 1$$

5. If $j < n$, go to 1.

II.5 Iterators

The major cost in computer time in a 4-body trajectory optimization problem is in function evaluation. Each function evaluation consists of the extrapolation of the state vector and the state transition matrix to the terminal time in multiple steps. The computation of cost and constraint gradients in terms of the terminal state and the state transition matrix is trivial.

The solution of the optimization problem will in general require several function evaluations. It is a difficult problem for two main reasons.

1). The problem is highly nonlinear. Only small variations from a reference trajectory is possible to insure convergence.

2). The cost function is often non-unimodal in a search direction. Any accelerated gradient method which requires an one-dimensional search must use some bracketing procedure to locate even a crude minimum in the search direction. A simple bracketing procedure will require several function evaluations. As a result, the cost in computer time in an one-dimensional search can easily become prohibitive.

During the early stage of the development considerable effort was spent in evaluating iterators which have been used successfully in solving 2-body trajectory optimization problems. Some qualitative comparisons of their effectiveness in solving the 3-body problems are given below.

II. 5. 1 Evaluation of Iterators

1. Jacobson-Oksman Method[7]

This is an accelerated gradient method, which was successfully used to optimize three and four-impulse two-body rendezvous trajectories[21]. It optimizes a scalar function using cubic fit interpolation in lieu of an one-dimensional search.

If there are constraints to be satisfied, they can be included only as a penalty function. The effectiveness of the method is reduced and the method cannot correct the general deficiency of the penalty function method.

This method was used to optimize cost in the outer loop of a 3-body 3-impulse transfer based on the classical formulation. The progress was very slow because the interpolated minimum falls very close to the starting point. Here, the advantage of not requiring an one-dimensional search appeared to be a disadvantage.

2. Fletcher-Powell Adaptation of Davidon's First Method[14, 15]

This is a popular accelerated gradient method to optimize a scalar function but it requires an one-dimensional search to be effective. The algorithm we tested came from a NASA MSC program "Optimum Multi-Impulse Rendezvous Program (OMIR)."[4] It incorporates an one-dimensional search method using a Golden Section bracketing procedure and cubic fit[20].

We tested it in the outer loop of a 3-body 3-impulse transfer. It was found that the iterator requires an excessive number of function

evaluations in the one-dimensional search. About 95% of the computer time is spent in this effort and the remaining small portion in updating the H-matrix and generating a new direction to proceed. The algorithm was satisfactory for the two-body problems where the Lambert problem can be solved in a single step and a large number of function evaluations is not particularly painful. The computation time can be reduced by a change of variables as suggested earlier but the ratio of time spent in one-dimensional search and that in generating a new direction will remain unchanged. The requirements of a one-dimensional search is a definite burden.

3. Campbell-Moore-Wolf Method[6]

This method is equivalent to the Armstrong-Marquadt Method[17, 18] in principle. The algorithm we tested came from the Princeton University program "Trajectory Optimization Program for Comparing Advanced Technologies (TOPCAT1)"[5]. It is also a penalty function method to handle constraints through internally generated weightings inversely proportional to the squares of the allowable tolerances. However, the user must supply proper scaling to keep numbers within computable range.

The step size and direction are controlled by an inhibitor, λ. When λ is very small, the method behaves like a Newton-Raphson method to satisfy the constraint. When λ is very large, the method behaves like a gradient method of a weighted scalar product of the constraint violations. The value of λ is increased when step size is exceeded or if the residual grows. It is reduced otherwise. In our test problems, λ has a steady tendency to grow such that not only the step direction is changed but also its magnitude is reduced. Neither characteristic is desirable since the user has no further control over the behavior once the mechanism for changing λ has been programmed and it is difficult to change λ in an optimal way.

The method has the inherent difficulties associated with a penalty

function method. Furthermore, one would normally desire to take gradient steps early in the process and then shift to the Newton-Raphson method. This method behaves just in the opposite manner. It is also very difficult to provide the proper scaling to be consistent with the desired tolerances and computable range.

4. Modified Fletcher Method

This is another version of Davidon's method proposed by Fletcher[24] and modified by Powers[23]. It still requires a crude one-dimensional search. In testing the method in the outer loop of a 3-impulse transfer it was found that a crude one-dimensional search as suggested by Powers did not work. The reason is that the function being optimized is often non-unimodal in the search direction. In order to achieve a cost reduction from the starting point it is necessary to use some kind of bracketing procedure such as one used in II.5.1.2. As a result, the number of function evaluation required becomes much larger than desired.

II.5.2 Recommended Iterators

A thorough evaluation of known iterators leads to the following selection of iterators.

1. No optimization

Newton-Raphson Method with a simple automatic step size control. This method will be used in 2 places.

1. Inner loop of a 3-impulse transfer
2. 2-impulse transfer from a point in space to earth.

2. Optimization only

Davidon's Second Method[16] This method does not require an one-dimensional search as in the Davidon's First Method[15]. It has the advantage of an accelerated gradient method without the penalty of excessive number of function evaluations. It appears to be the most efficient method among the ones tested. It will be used in:

1. The outer loop of a 3-impulse transfer
2. A 2-impulse transfer from the earth to a point in conjunction with the gradient projection method.

3. Optimization with Constraints

1. Gradient Projection Method[22] This method will be used to generate fuel-optimal two-impulse trajectories from the earth to a point in space for a fixed transfer time.

2. Accelerated Gradient Projection Method[19, 25] This is a accelerated version of the gradient projection method. It is a combination of the standard gradient projection method and an accelerated gradient method. The Davidon's Second method will be used for the accelerated gradient portion of the algorithm. It will be used as a replacement of the gradient projection method if feasible.

II.6 An Example of a Four-Body Two-Impulse Transfer

An example of a 4-body 2-impulse trajectory from the L_1 libration point to the earth has been generated. The transfer time is 116.682 days which is the same as the typical loop type 3-body trajectory mentioned in Part I. This a a 3-dimensional problem. Both the earth and the moon have initial position and velocity components normal to the ecliptic. The projection of the trajectory with respect to the earth in a plane parallel to the ecliptic is shown in Fig. 22. The 3-body trajectory of the same transfer time is shown in Fig. 24. It is evident that the 4-body trajectory is noticeably different from the 3-body trajectory. The presence of the moon as a separate entity appears to have a very strong effect on the trajectory. The distances of the vehicle from the earth and the moon is shown as a function of time in Fig. 25. There are three intervals during which the vehicle is closer to the moon than the earth. The mass ratios used are shown in Appendix A. The initial conditions of the earth and the moon were obtained from a MAC data file on JPL Development Ephemeris No. 69.

The primer vector history of this 4-body trajectory is shown in Fig. 23. It is a fuel-optimal 2-impulse transfer for the initial conditions used. A search for the optimal initial conditions has not been done.

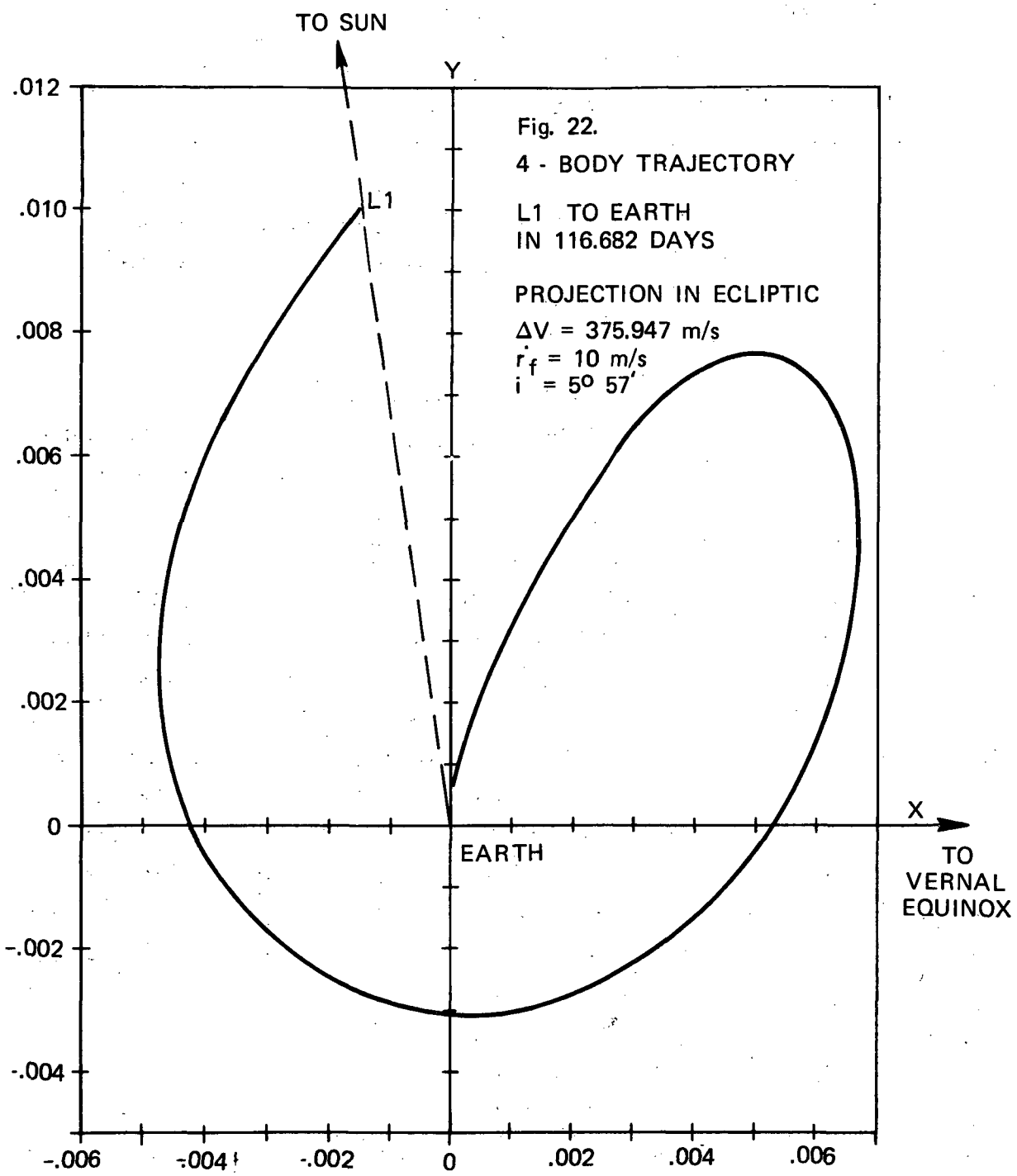
TO SUN
Y
.012
.010
.008
.006
.004
.002
0
-.002
-.004
-.006
-.004
-.002
0
.002
.004
.006
L1
EARTH
X
TO
VERNAL
EQUINOX
Fig. 22.
4 - BODY TRAJECTORY
L1 TO EARTH
IN 116.682 DAYS
PROJECTION IN ECLIPTIC
ΔV = 375.947 m/s
$\dot{r}_f$ = 10 m/s
i = 5° 57'

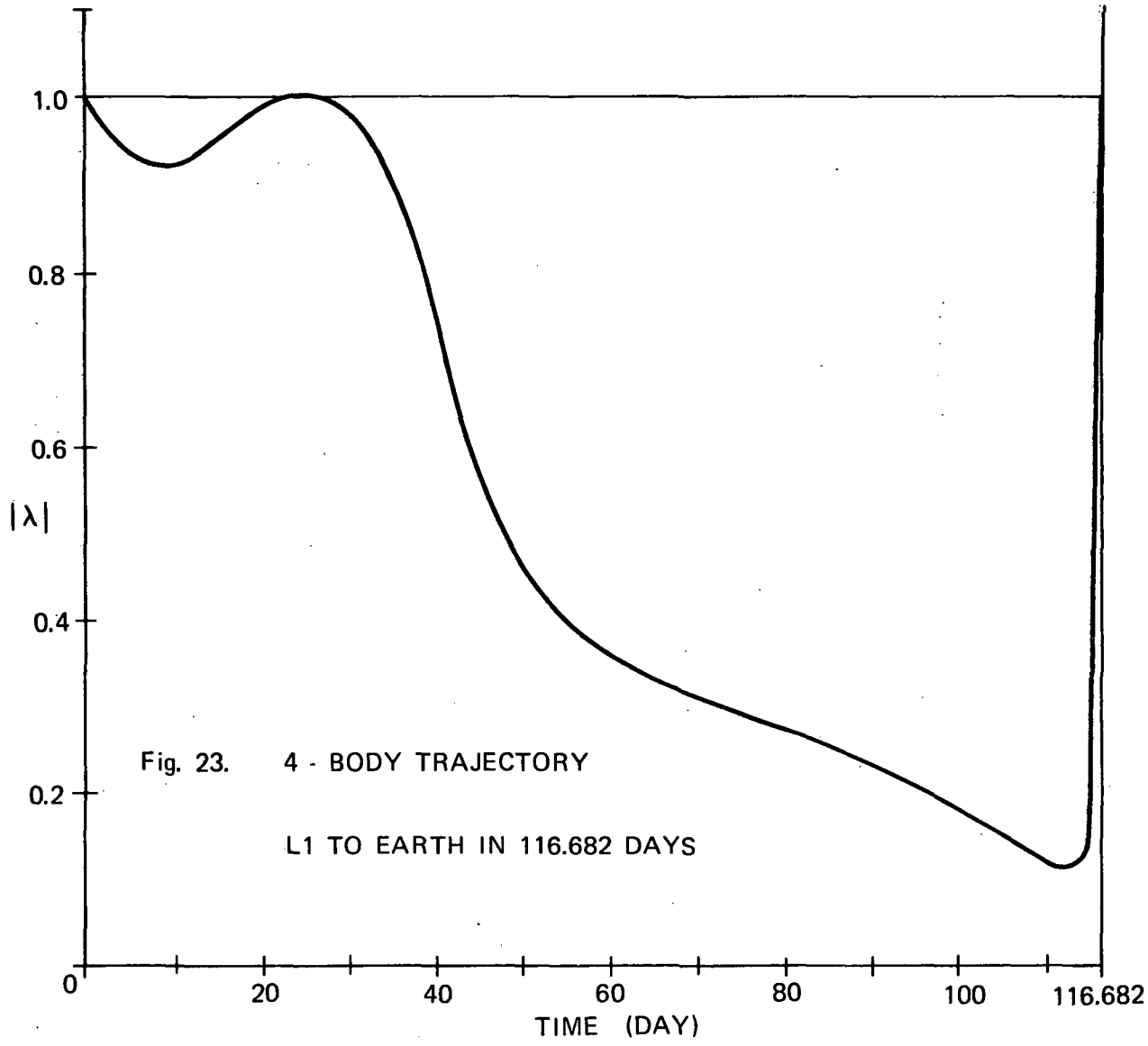

Fig. 23. 4 - BODY TRAJECTORY

L1 TO EARTH IN 116.682 DAYS

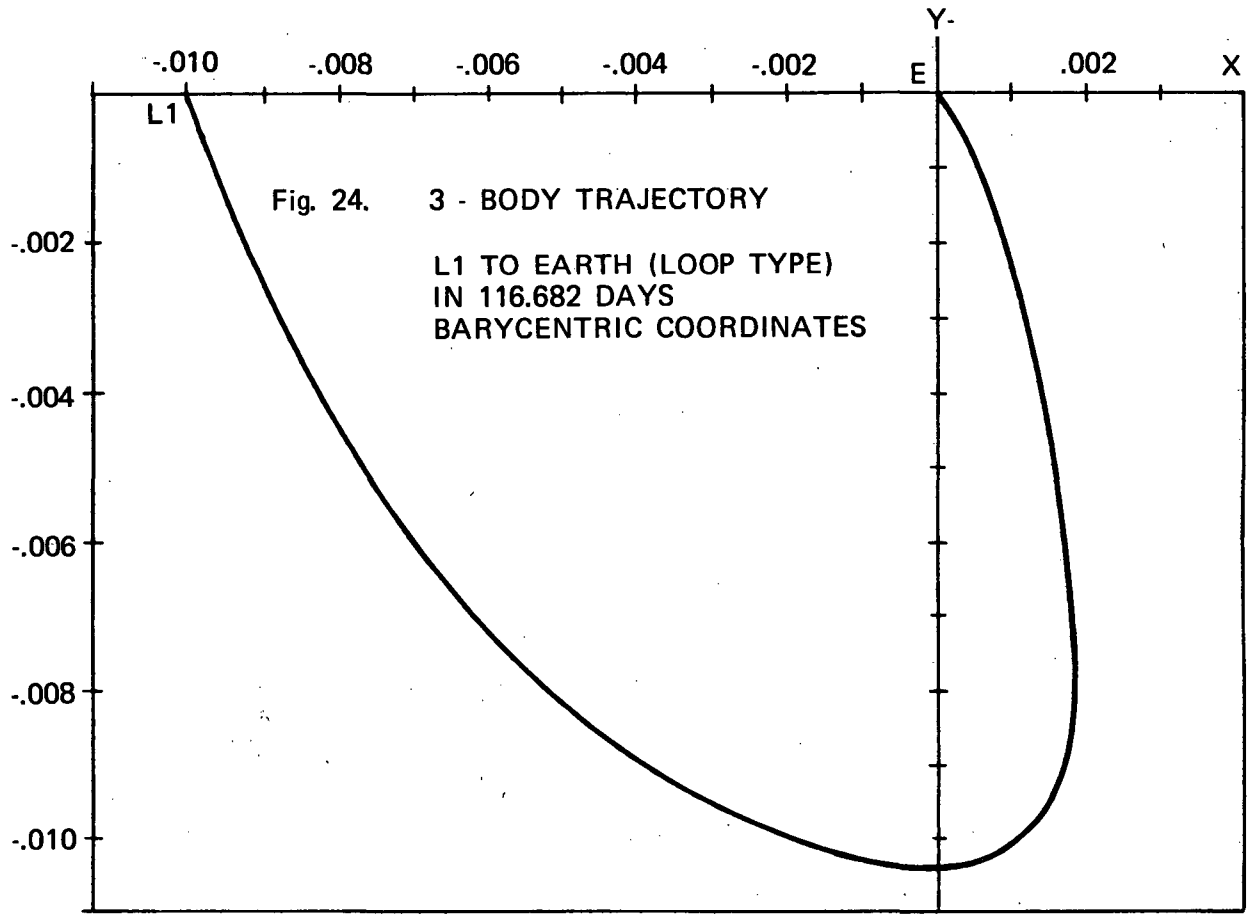

Fig. 24. 3 - BODY TRAJECTORY

L1 TO EARTH (LOOP TYPE)
IN 116.682 DAYS
BARYCENTRIC COORDINATES

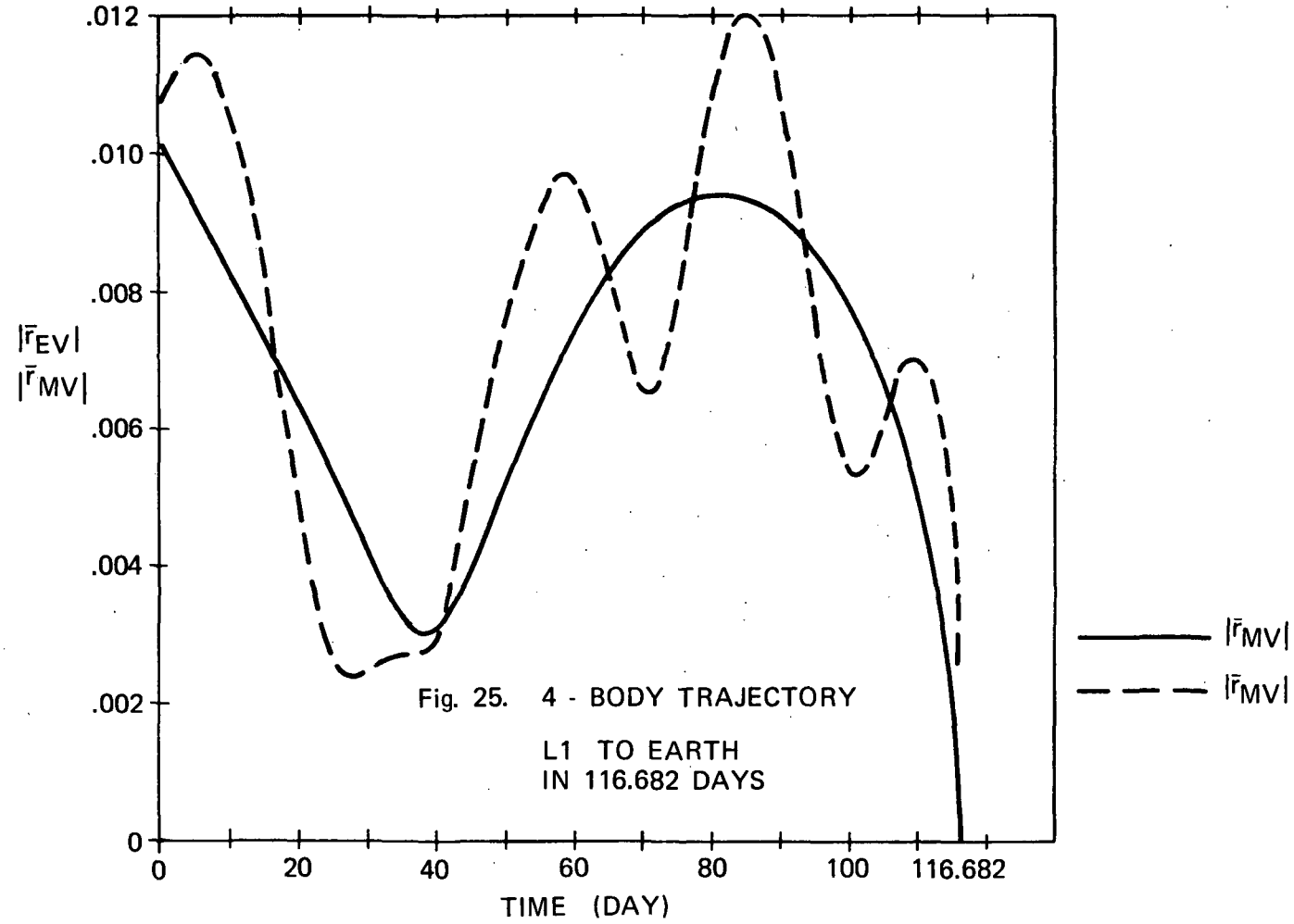

Fig. 25. 4 - BODY TRAJECTORY

L1 TO EARTH
IN 116.682 DAYS

REFERENCES

1. D'Amario, L. and T. N. Edelbaum, "Minimum Impulse Three-Body Trajectories," MIT C. S. Draper Laboratory Report No. R-723, July 1972.

2. Lion, P. M. and M. Handelsman, "Primer Vector on Fixed Time Impulsive Trajectories," AIAA Journal, Vol. 6, No. 1, Jan. 1968.

3. Jezewski, D. J. and H. L. Rozendaal, "An Efficient Method for Calculating Optimal Free-Space N-Impulse Trajectories," AIAA Journal, Vol. 6, No. 11, Nov. 1968.

4. Rozendaal, H. L., A. G. Onley and D. R. Glandorf, "Computer Program Documentation - Optimum Multi-Impulse Rendezvous Program (OMIR)," Report No. 672-25-AX125, Lockheed Electronics Co., Houston, Texas, July 1968.

5. Lion, P. M., J. H. Campbell and A. B. Shulzycki, "Trajectory Optimization Program for Comparing Advanced Technologies (TOPCAT1)," Aerospace Engineering Report No. 717s, Princeton University, Princeton, N. J., March 1968.

6. Campbell, J. H., W. E. Moore and H. Wolf, "A General Method for Selection and Optimization of Trajectories," Progress in Astronautics and Aeronautics, Vol. 17, 1966.

7. Jacobson, D. and W. Oksman, "An Algorithm that Minimizes Homogeneous Functions of N Variables in N + 2 Iterations and Rapidly Minimize General Functions," Harvard University, Div. of Engineering and Applied Physics, Tech. Report No. 618, Oct. 1970.

8. Wilson, S. W., "A Pseudostate Theory for The Approximation of Three-Body Trajectories," AIAA Paper 70-1061, Aug. 1970.

9. Byrnes, D. V. and H. L. Hooper, "Multi-Conic: A Fast and Accurate Method of Computing Space Flight Trajectories," AIAA Paper 70-1062, Aug. 1970.

10. Stumpff, K. and E. H. Weiss, "Applications of an N-Body Reference Orbit," Journal of the Astronautical Sciences, Vol. 15, No. 5, Sept.-Oct. 1968.

11. Weiss, E. H., "A New Method for Computing the State Transition Matrix," Journal of the Astronautical Sciences, Vol. 16, No. 3, May-June 1969.

12. Stumpff, K. and E. H. Weiss, "A Fast Method of Orbit Computation," NASA TN D-4470, Oct. 1967.

13. Goodyear, W. H., "A General Method for the Computation of Cartesian Coordinates and Partial Derivatives of the Two-Body Problem," NASA CR-522, Sept. 1966.

14. Fletcher, R. and M. J. D. Powell, "A Rapidly Convergent Descent Method for Minimization," The Computer Journal, Vol. 6, No. 2, July 1963.

15. Davidon, W. C., "Variable Metric Method for Minimization," ARC Research Development Report ANL-5990 Rev. 1959.

16. Davidon, W. C., "Variance Algorithm for Minimization," The Computer Journal, Vol. 10, No. 4, Feb. 1968.

17. Armstrong, E. S., "A Combined Newton-Raphson and Gradient Parameter Correction Technique for Solution of Optimal Control Problems," NASA TR R-293, 1968.

18. Marquardt, D. W., "An Algorithm for Least-Squares Estimation of Non-Linear Parameters," J. SIAM, Vol. 11, No. 2, June 1963.

19. Kelley, H. J. and J. L. Speyer, "Accelerated Gradient Projection," Lecture Notes in Mathematics 132, Symposium on Optimization, Spinger,Verlag, Berlin, 1970.

20. Johnson, I. L., Jr., and G. E. Meyers, "One-Dimensional Minimization using Search by Golden Section and Cubic Fit Method," NASA MSC Internal Note No. 67-FM-172, Nov. 1967.

21. Pu, C. L., "On Primer Vector Theory and Rendezvous Targeting," 23A STS Memo No. 53-71 Rev. 1, MIT C. S. Draper Laboratory, Jan. 1972.

22. VanderVelde, W. E., "Class Note on Applied Optimal Control," MIT Course No. 16.39T, Department of Aeronautics and Astronautics, Feb. 1967.

23. Powers, W. F., "A Crude Search Davidon-Type Technique with Application to Shuttle Optimization, AIAA Paper No. 72-907, Sept. 1972.

24. Fletcher, R., "A New Approach to Variable Metric Algorithms," Computer Journal, Vol. 13, No. 3, 1970.

25. Pu, C., "An Accelerated Gradient Projection Method Using Davidon's Variance Algorithm," I0 E SGA Memo No. 1-73 (Rev. 1), The C. S. Draper Laboratory, 4 Oct. 1973.

APPENDIX A

Three-Body Space

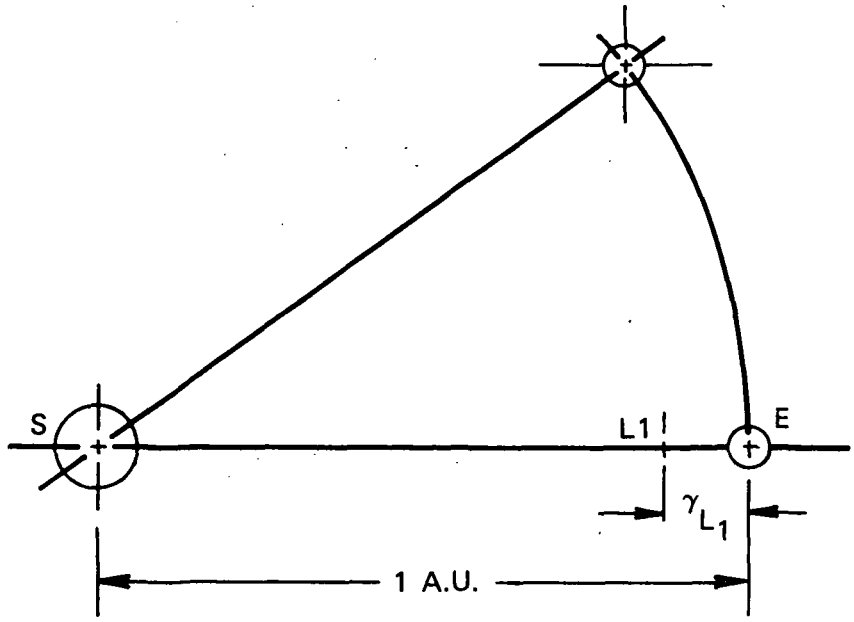

1 A. U. = 1.49597893×10^{8} KM

$\gamma_{L_1} = 1.001098 \times 10^{-2}$

$\mu_{E+M} = 3.0404322 \times 10^{-6}$

$\mu_{S} = 9.9999696 \times 10^{-1}$

Four-Body Space

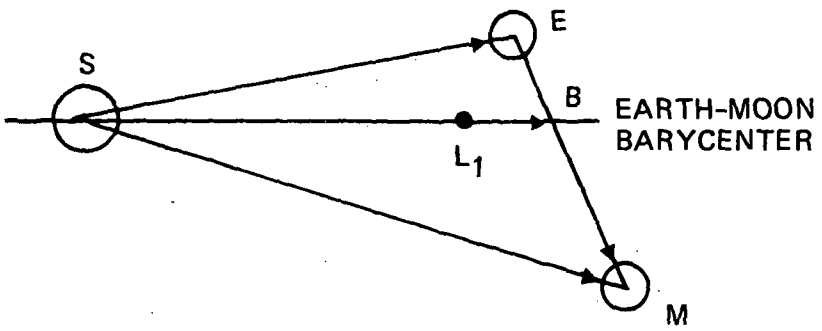

$$\overline{r}_{SB} = \overline{r}_{SE} + \frac{\mu_M}{\mu_E + \mu_M}\,\overline{r}_{EM}$$

$$\overline{r}_{SL_1} = (1 - \gamma_{L_1})\,\overline{r}_{SB}$$

$$\overline{V}_{SB} = \overline{V}_{SE} + \frac{\mu_M}{\mu_E + \mu_M}\,\overline{V}_{EM}$$

$$\overline{V}_{SL_1} = (1 - \gamma_{L_1})\,\overline{V}_{SB}$$

$$\gamma_{L_1} = 1.001098 \times 10^{-2}$$

$$\left.\begin{aligned} \mu_E &= 3.0034845 \times 10^{-6} \\ \mu_M &= 3.6943122 \times 10^{-8} \\ \mu_S &= 9.9999696 \times 10^{-1} \end{aligned}\right\}$$

Based on mass ratios from JPL Tech. Report 32-1306.

APPENDIX B

Accelerations

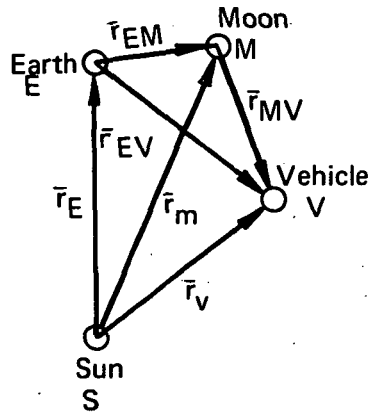

$$\ddot{\bar{r}}_S = \mu_E \frac{\bar{r}_E}{r_E^3} + \mu_M \frac{\bar{r}_M}{r_M^3}$$

$$\ddot{\bar{r}}_E = -\mu_S \frac{\bar{r}_E}{r_E^3} + \mu_M \frac{\bar{r}_{EM}}{r_{EM}^3}$$

$$\ddot{\bar{r}}_M = -\mu_S \frac{\bar{r}_M}{r_M^3} - \mu_E \frac{\bar{r}_{EM}}{r_{EM}^3}$$

$$\ddot{\bar{r}}_V = -\mu_S \frac{\bar{r}_V}{r_V^3} - \mu_E \frac{\bar{r}_{EV}}{r_{EV}^3} - \mu_M \frac{\bar{r}_{MV}}{r_{MV}^3}$$

Relative motion:

$$\ddot{\bar{r}}_{SV} = -\mu_S \frac{\bar{r}_V}{r_V^3} - \mu_E \left(\frac{\bar{r}_{EV}}{r_{EV}^3} + \frac{\bar{r}_E}{r_E^3}\right) - \mu_M \left(\frac{\bar{r}_{MV}}{r_{MV}^3} + \frac{\bar{r}_M}{r_M^3}\right)$$

$$\ddot{\bar{r}}_{EV} = -\mu_S \left(\frac{\bar{r}_V}{r_V^3} - \frac{\bar{r}_E}{r_E^3}\right) - \mu_E \frac{\bar{r}_{EV}}{r_{EV}^3} - \mu_M \left(\frac{\bar{r}_{MV}}{r_{MV}^3} + \frac{\bar{r}_{EM}}{r_{EM}^3}\right)$$

$$\ddot{\bar{r}}_{MV} = -\mu_S\left(\frac{\bar{r}_V}{r_V^3} - \frac{\bar{r}_M}{r_M^3}\right) - \mu_E\left(\frac{\bar{r}_{EV}}{r_{EV}^3} - \frac{\bar{r}_{EM}}{r_{EM}^3}\right) - \mu_M\frac{\bar{r}_{MV}}{r_{MV}^3}$$

$$\ddot{\bar{r}}_{SE} = -\left(\mu_S + \mu_E\right)\frac{\bar{r}_E}{r_E^3} + \mu_M\left(\frac{\bar{r}_{EM}}{r_{EM}^3} - \frac{\bar{r}_M}{r_M^3}\right)$$

$$\ddot{\bar{r}}_{SM} = -\left(\mu_S + \mu_M\right)\frac{\bar{r}_M}{r_M^3} - \mu_E\left(\frac{\bar{r}_{EM}}{r_{EM}^3} + \frac{\bar{r}_E}{r_E^3}\right)$$

$$\ddot{\bar{r}}_{EM} = -\mu_S\left(\frac{\bar{r}_M}{r_M^3} - \frac{\bar{r}_E}{r_E^3}\right) - \left(\mu_E + \mu_M\right)\frac{\bar{r}_{EM}}{r_{EM}^3}$$

Distribution:

NASA Scientific and Technical Information Facility (5)

NASA Headquarters

MTE/V. N. Huff

SM/R. Allenby

Goddard Space Flight Center

581/R. Coady

581/R. Farquhar (10)

580/R. Groves

661/T. Von Rosenving

701/J. Madden

C. S. Draper Laboratory

R. H. Battin

S. R. Croopnick

L. D'Amario

J. C. Deckert

T. N. Edelbaum (10)

D. C. Fraser

D. G. Hoag

G. M. Levine

R. V. Ramnath

L. L. Sackett

J. L. Speyer

C. Pu (10)

M. I. T.

J. J. Deyst

W. Markey